

**Master in Chemical Engineering**

***Modeling of oligomerization in C<sub>3</sub>-cut selective hydrogenation***

**A Master's dissertation**

of

**Bruno Miguel Queirós Rola Teixeira**

**Developed within the course of dissertation**

held in

**IFP Energies Nouvelles**



Supervisor at FEUP: **Prof. José Miguel Loureiro**

Supervisor at IFP Energies Nouvelles: **Dr. Adrien Mekki-Berrada**



**Departamento de Engenharia Química**

**October of 2018**



## Acknowledgment

I started this thesis in Lyon (France), I continued it in Porto (Portugal), and I finished it in Eindhoven (the Netherlands). Those are the three places that defined my higher education of 5 years in Chemical Engineering, and I would like to thank to everyone that contributed to it.

To start, reaching this point would not be possible without my parents that always supported me in all my ambitious adventures, and only due to their hard work in life I was able to have the chance to dream further.

I want to thank and dedicate my thesis to my grandparents, since they believed in my abilities during all my life, and no one is happier than them with the accomplishment of my Engineer degree.

I want to thank to my tutors Adrien Mekki-Berrada and Prof. Loureiro for their patience and all the knowledge that I add the pleasure to acquire with them.

To the Pinto de Macedo family, that taught me and showed me the true meaning of never forgetting our own roots. I will always have a big family in Lyon.

A big thanks to my Diana for her patience during my master thesis and also for her help in how to beautify this document. To all my friends that I made in these 5 years, in special to the international group of interns that we add at IFPen. With them, every failure and frustration of this project seemed meaningless whenever they were around providing their good disposition, friendship and love. I want to thank to my closest friends from FEUP, that despite me being away a total amount of time of 1 year, never lost their affection and their friendship for me. Also to my friends from my hometown Maia, that followed different paths than mine but were still always able to be an immense part of my life.

I want also to thank to my lab partner Elodie Dusson, to my laboratory coach and Jedi Master Serge Boivineau, and to Nicolas Laloue for his kind words that would relive me in stressful situations.

To the European Union that it is the best project that I will ever be able to experience.

Prof. José Miguel Loureiro, supervisor of this work, is a member of the Associate Laboratory LSRE-LCM, Project POCI-01-0145-FEDER-006984, funded by FEDER through COMPETE2020 - Programa Operacional Competitividade e Internacionalização (POCI) - and by national funds through FCT - Fundação para a Ciência e a Tecnologia.



## Abstract

The oligomerization of the C<sub>3</sub>-cut in the selective hydrogenation of methylacetylene and propadiene (commonly referred as MAPD) is a major drawback of the whole process, since it decreases the run time of the expensive catalyst by deactivating it. This thesis focus particularly on the liquid phase configuration of this process and has the intention to acquire more knowledge about it due to the lack of information in the public domain of this event.

Throughout this project several experimental tests were performed in a batch reactor and from two different sampling procedures and four different analytic tools, the quantification of the produced oligomers was carried out. The sampling balloons allowed the quantification of the oligomers from C<sub>6</sub> to C<sub>8</sub> by means of a gas chromatograph, and the quantification of the hydrogen composition inside the reactor with other gas chromatograph. The produced green-oil was dissolved with n-heptane and analyzed via gas chromatography-mass spectrometry. The used catalyst was collected and analyzed with thermogravimetric analysis.

In the end of this project, it was possible to identify 16 different oligomers from C<sub>6</sub> to C<sub>8</sub> and divide them in 5 distinct populations. Two different mechanisms were proposed that take into account the oligomerization of the C<sub>3</sub>-cut.

**Keywords (theme):**

Oligomerization, green-oil, C<sub>3</sub>-cut, MAPD, selective hydrogenation, liquid phase

---



## Declaration

I hereby declare, on my word of honour, that this work is original and that all non-original contributions were properly referenced with source identification.

Porto, 1<sup>st</sup> of October 2018

A handwritten signature in blue ink that reads "Bruno Miguel Queirós Rola Teixeira". The signature is written in a cursive style.

(Bruno Miguel Queirós Rola Teixeira)

---

# Index

<b>1</b>	<b>Introduction.....</b>	<b>1</b>
1.1	Framing and presentation of the work .....	1
1.2	Contributions of the Work.....	2
1.3	Organization of the thesis.....	2
<b>2</b>	<b>Context and State of the art.....</b>	<b>3</b>
<b>3</b>	<b>Materials and Methods .....</b>	<b>7</b>
<b>3.1</b>	<b>Experimental.....</b>	<b>7</b>
3.1.1	Catalyst .....	7
3.1.2	C <sub>3</sub> -cut Feed.....	7
3.1.3	U865 Unit .....	8
3.1.4	H <sub>2</sub> /N <sub>2</sub> Ballast .....	10
3.1.5	Procedure .....	11
3.1.6	Operating Conditions .....	19
<b>3.2</b>	<b>Analysis .....</b>	<b>20</b>
3.2.1	GC Alumina Bond (“GC AB”) .....	20
3.2.2	GC used for estimating H <sub>2</sub> and N <sub>2</sub> .....	24
3.2.3	Thermogravimetric Analysis (TGA).....	27
3.2.4	Gas Chromatography-Mass Spectrometry (GC-MS) .....	28
<b>4</b>	<b>Results .....</b>	<b>29</b>
4.1	Mass balance: how to consider it for oligomers.....	29
4.2	Test 1 - standard hydrogenation conditions .....	30
4.3	Test 2.....	31
4.4	Test 3.....	32
4.5	Test 4.....	33
4.6	Tests 5 and 6.....	34
4.7	Tests 7 and 8.....	35
4.8	Tests 9 and 10 .....	36

4.9	Test 11 .....	38
4.10	Test 12 .....	39
4.11	Tests 13 and 14 .....	40
5	Discussion .....	42
6	Conclusion.....	48
7	Assessment of the work done .....	49
7.1	Objectives Achieved.....	49
7.2	Other Work Carried Out .....	49
7.3	Limitations and Future Work .....	49
7.4	Final Assessment.....	49
	References .....	50
Appendix 1	Rescaled results of GC AB and GC H <sub>2</sub> .....	51
Appendix 2	Photography of green-oil and catalyst .....	58

---

## Notation and Glossary

P	Pressure	bar
rpm	Rotations per minute	
T	Temperature	°C

### *List of Acronyms*

CP	Cyclopropane
EI	Electron Ionization
ET	Ethane
FID	Flame Ionization Detector
G/L	Gas/Liquid
GC	Gas Chromatogram
GC-MS	Gas Chromatogram-Mass Spectroscopy
GS	Grayson-Streed
HC	Hydrocarbon
MA	Methylacetylene
MAPD	Methylacetylene and Propadiene
PD	Propadiene
PE	Propylene
PN	Propane
SRK	Soave-Redlich-Kwong
STP	Standard Temperature and Pressure
TCD	Thermal Conductivity Detector
TGA	Thermogravimetric Analysis

# 1 Introduction

## 1.1 Framing and presentation of the work

The steam cracking is an industrial petrochemical process that resorting high temperatures and high pressures, breaks down long saturated hydrocarbon molecules in smaller ones, often unsaturated. The composition of this outlet stream depends heavily on the crude hydrocarbon inlet's nature and on the intensity of the cracking process. In all its possible varieties, one gas light fraction that is commonly present is the C<sub>3</sub> fraction. After distillation processes it is possible to isolate this C<sub>3</sub>-cut from the other hydrocarbon cuts. The C<sub>3</sub>-cut is still not a homogenous stream, since it consists normally in 90% of propylene, 5% of methylacetylene (MA) and propadiene (PD) and about 5% of propane. From propylene it's possible to obtain, through polymerization processes, polypropylene, a plastic massively produced worldwide. However, for doing so, the inlet C<sub>3</sub>-stream must contain a maximum of 2 ppm of MA and PD, or MAPD, in order to avoid poisoning of the polymerization catalysts. Through a downstream distillation process, the propane can be removed from the C<sub>3</sub>-cut while the separation of the polyunsaturated compounds (MAPD) from the propylene is unfeasible in this process due to the similarity of the boiling points of these three compounds. For the removal of the MAPD traces, a selective hydrogenation process takes place, converting MAPD into propylene. This process may have two different configurations: the front end hydrogenation, in the case that the hydrogenation takes place before the separation unit; and the tail end hydrogenation, in the case that it occurs after. In this separation process H<sub>2</sub>, CH<sub>4</sub>, CO and some eventual small fraction of C<sub>2</sub> compounds are removed from the C<sub>3</sub>-cut. Since the selective hydrogenation of MAPD is the desired reaction in this process, it is very important in this process to regulate the right operating conditions in order to maximize the selectivity towards propylene. Otherwise, there will be an over-hydrogenation of the molecules, producing propane, which is unwanted since it is a product with a lower market value. The over-hydrogenation of propylene can also be dangerous since it is a highly exothermic reaction, which can provoke a run-away reaction. The selective hydrogenation of MAPD can occur either in the gas phase, or in the liquid phase. The liquid phase hydrogenation of MAPD is a relatively new technology introduced in industry, and it is believed to increase the catalyst life by removing with the liquid flow, the carbonaceous deposits formed during the process. Industrially for this purpose, fixed bed catalytic reactors are used, and as for the catalyst, palladium active sites over alumina support are the most commonly used. The carbonaceous deposits formed in this process are oligomers formed in the reactor that deposit over the catalyst surface leading to its deactivation. One operating condition that seems to heavily influence this side reaction is the H<sub>2</sub>/MAPD ratio. The

oligomerization of the C<sub>3</sub>-cut, particularly in the liquid phase, is still a new topic in the scientific community, and this Master thesis is focused on it.

## 1.2 Contributions of the Work

This project focuses on modelling the oligomerization reactions of the C<sub>3</sub>-cut selective hydrogenation, and for doing so, extensive data needs to be gathered at first from experimental work. The experimental unit U865 had already been used for testing the feasibility of this project, and it showed to be a good tool for carrying out this process.

I studied the operating conditions in a simulator of the hydrogenation of the C<sub>3</sub>-cut, and the most satisfactory ones were chosen to be reproduced in the laboratory. After being acquainted with the experimental and analytic set-up, I carried out several tests in a batch reactor and the samples collected were analyzed in 2 gas chromatographs, with thermogravimetric analysis and with gas chromatography-mass spectrometry technique.

After I treated the data, two reaction mechanisms were proposed and some modelling work was started.

## 1.3 Organization of the thesis

After the introductory chapter, where the framework and presentation of the project are done, this master thesis has the following organization by chapters:

Chapter 2- Context and State of the art: in this chapter, the scientific literature available on the topic and similar ones, is reviewed.

Chapter 3- Materials and Methods: this chapter includes the presentation of the catalyst, the C<sub>3</sub>-cut feed, the experimental unit, the procedures and the analytic tools used in the project.

Chapter 4- Results: here the results obtained by the experimental set-up described before, are exposed.

Chapter 5- Discussion: the results presented previously are discussed.

Chapter 6- Conclusion: all the conclusions that were drawn during this project are presented.

Chapter 7- Assessment of the work done: In this last chapter, a global balance of the project is done, as well as the presentation of proposals for future works.

## 2 Context and State of the art

Due to the non-existence of knowledge, in the public domain, of the oligomerization of MAPD in the liquid phase, two different tactics were opted in order to give the best possible understanding of the phenomena. After searching for information about the actual topic, two similar topics were also searched for: the oligomerization of MAPD in the gas phase; and the oligomerization of the C<sub>2</sub>-cut. This latter reaction occurs always in gas phase since there are no available technologies that condensate the C<sub>2</sub> molecules in the petrochemical industry. Wang and Froment (2005) proposed a kinetic model for the C<sub>3</sub>-cut selective hydrogenation in the gas phase and its numerical simulation in a fixed bed reactor. A Pd metal catalyst supported on alumina is tested at temperatures of 60 °C and 80 °C. In their kinetic scheme and equations, they take into account the green-oil (oligomeric products) formation up until compounds with 9 carbons. By resorting their two on-line gas chromatograms, no chemical nature of these oligomers was reported, as well as no distinction on the kinetics of the formation of different oligomers with the same carbon number. Wang and Froment proposed 2 mechanisms, depending on whether the propylene also oligomerize or not. The mechanisms are schematized in Figure 2.1 a) and b):

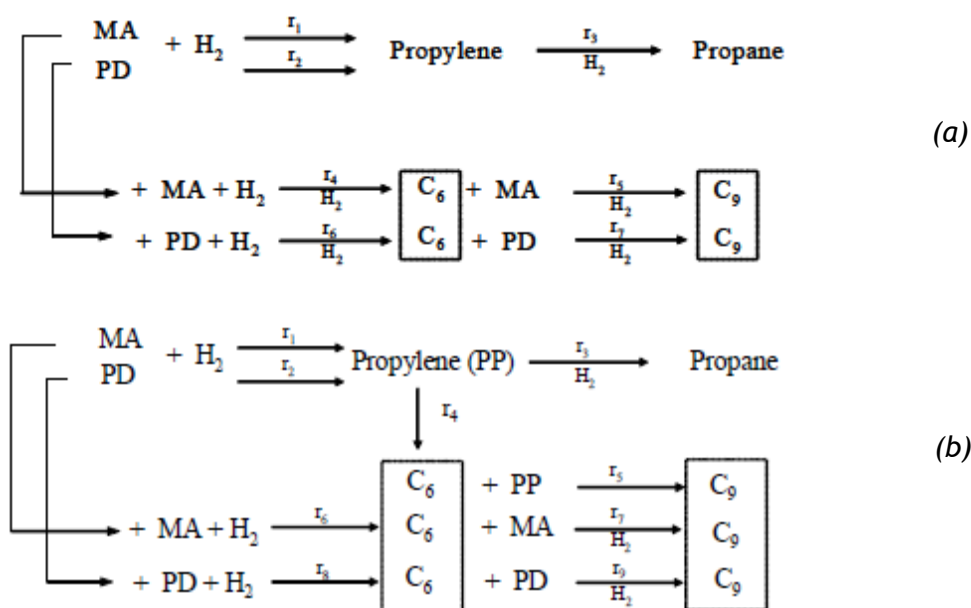


Figure 2.1 - a) and b) schemes of reacting mechanisms proposed in Wang and Froment (2005).

In Bond and Sheridan (1952) on the study of the selective hydrogenation of propadiene gas on palladium and platinum-based catalysts, it was already reported the formation of oligomer residues during the reaction, especially over palladium catalysts. They suggest that a Van der Waals layer of propadiene, over a chemisorbed layer, is responsible for the oligomerization side

reactions. It's also referred that propadiene adsorbs with more strength than propylene on the metal active sites.

McCue et al.(2016), studied the hydrogenation of the C<sub>3</sub>-cut over palladium assisted copper/alumina catalysts. The selectivities towards propylene, propane and oligomers were investigated by changing the copper/palladium atomic ratios in the catalysts. One of the conclusions of this report is that catalysts with a higher copper content tend to produce more oligomers (i.e. higher selectivity towards oligomers). Their interpretation of this evidence is that at lower temperatures, hydrogen gas will not adsorb so much on the Cu sites, but rather on the Pd sites. By increasing the temperature, the hydrogen adsorption on the Cu sites can be improved, which leads to results with lower oligomer selectivity. Meaning that oligomers are more propitious to form under conditions of limited dissociation of hydrogen. Similar conclusions are also drawn by Bridier et al. (2010).

In the oligomerization of MAPD molecules, there might happen two scenarios: a homo-oligomerization, in the case when a MA (or PD) molecule reacts with one of its kind (Figure 2.2 a)); and a co-oligomerization, in the case when a MA molecule reacts with a PD molecule (Figure 2. 2 b)). Eventually, if propylene also oligomerizes with MAPD it will result in a co-oligomer.

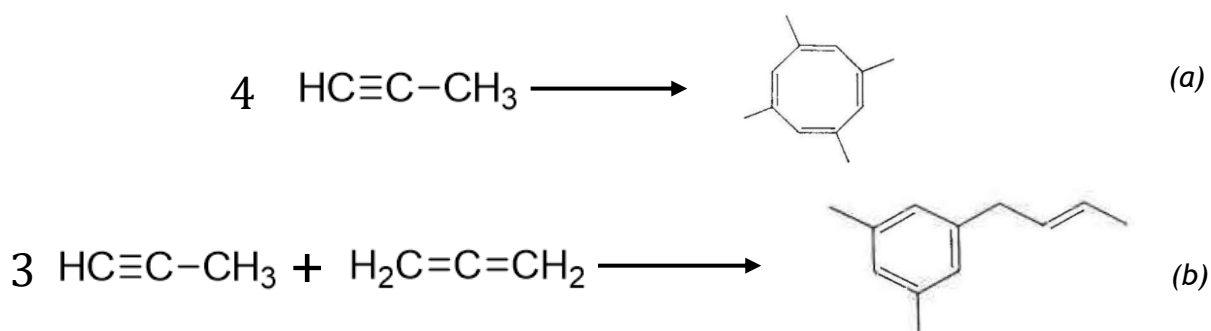


Figure 2.2 - a) homo-oligomerization and b) co-oligomerization examples.

Since both of monomers are molecules containing 3 carbon atoms, their oligomers will contain a number of carbons that is a multiple of 3. In the case illustrated above, a compound with 12 carbon atoms (tetramer) is produced from 4 monomers. When two molecules oligomerize, the outcome product will be called a dimer. In the case of 3 molecules, it will be called a trimer, and so on. Despite the monomers of this reaction will produce oligomers with a carbon number that is a multiple of 3, some other products with different number of carbons can be produced in the case that occurs the oligo-cracking as another side reaction, breaking the molecule into smaller ones.

Concerning the chemical nature of the formed oligomers, one study is worth mentioning. Čermák et al. (1988), studied the co-oligomerization reaction between MA and PD in nickel complexes as well as the homo-oligomerization reactions, using radioactivity tracking. They

were able to identify 43 different oligomers containing until 15 carbons (pentamers), the majority of them being aromatic compounds, and others being cyclic olefins.

Reading about the oligomerization of C<sub>2</sub> compounds can also lead to a better understanding of the discussed topic. Borodziński and Cybulski (2000) proposed a kinetic model for the hydrogenation of acetylene-ethylene mixtures over a Pd/Al<sub>2</sub>O<sub>3</sub> catalyst covered by carbonaceous deposits, i.e. oligomers. They propose the existence of 3 different active sites on the surface of the catalyst that differentiate between them in the size of the active site. The two smallest sites represent small palladium spaces in between carbonaceous spaces deposited on a palladium surface, and only acetylene and hydrogen can be adsorbed there. The acetylene molecule adsorbs perpendicularly whereas the ethylene molecule cannot since it needs larger spaces to do so. In the largest of the active sites, all the three molecules have enough space to be adsorbed, thus these sites are the ones responsible for the unwanted hydrogenation of ethylene into ethane (the same principle already explained as for the C<sub>3</sub>-cut).

Another classification of the different types of active sites is based on the acidity of the site. The studies of Wang and Froment (2005), and Mary et al. (2016), are based on the premise that the metal sites of the catalyst are responsible for the hydrogenation of MAPD and propylene, whereas the acid sites are responsible for the oligomerization.

In the review paper of Bos and Westerterp (1993) there is a report of a 1993 study on the kinetics and mechanisms of ethyne and ethane selective hydrogenation. Once again it is affirmed that the production of oligomers is mainly controlled by the ratio of H<sub>2</sub>/C<sub>2</sub>H<sub>2</sub>. It seems that increasing the ratio content inhibits the oligomer formation, however due to an unknown effect, no oligomerization occurs in the absence of hydrogen.

On a different note, it is also worth to mention that some novel reactor technologies are being studied and developed in order to improve industrially the selective hydrogenation of MAPD, such as Pd/Al<sub>2</sub>O<sub>3</sub> catalysts coated with an ionic liquid layer in Friedrich et al. (2017) and a catalytic membrane reactor in Teixeira et al. (2011).



## 3 Materials and Methods

### 3.1 Experimental

#### 3.1.1 Catalyst

The catalyst used for the set of experiments is a commercial sample produced by Axens SA. This catalyst is composed by some palladium active sites dispersed over an alumina support and it is used industrially in various selective hydrogenation processes such as: liquid phase purification of a C<sub>3</sub>-cut stream by hydrogenation of propyne and propadiene into propylene; liquid phase selective hydrogenation of butadiene; and hydrogenation of diolefins for the stabilization of pyrolysis gasoline. The catalyst particles can be seen in Figure 3.1:



Figure 3.1 - Photography of the catalyst particles of Pd/Al<sub>2</sub>O<sub>3</sub>.

#### 3.1.2 C<sub>3</sub>-cut Feed

The C<sub>3</sub>-cut feed used in this project has the following composition (Table 3.1):

Table 3.1 - C<sub>3</sub>-cut composition.

Compound	Acronym	wt%
Ethane	ET	0.06
Propane	PN	3.94
Cyclopropane	CP	0.04
Propylene	PE	93.66
Propadiene	PD	1.02
Propyne	MA	1.28

When compared to the typical industrial values, the MAPD concentration in this feed is lower than the usual. This fact can be explained in the case that this feed comes from a reactor with recycle, in which the MAPD is diluted with the recycled stream with lower MAPD content.

### 3.1.3 U865 Unit

The unit in which the experiments were carried out is composed of 4 major parts: the reactor, the C<sub>3</sub> “grayel” bottle, the ballast containing hydrogen and nitrogen and the control panel. The unit can be seen in Figure 3.2:

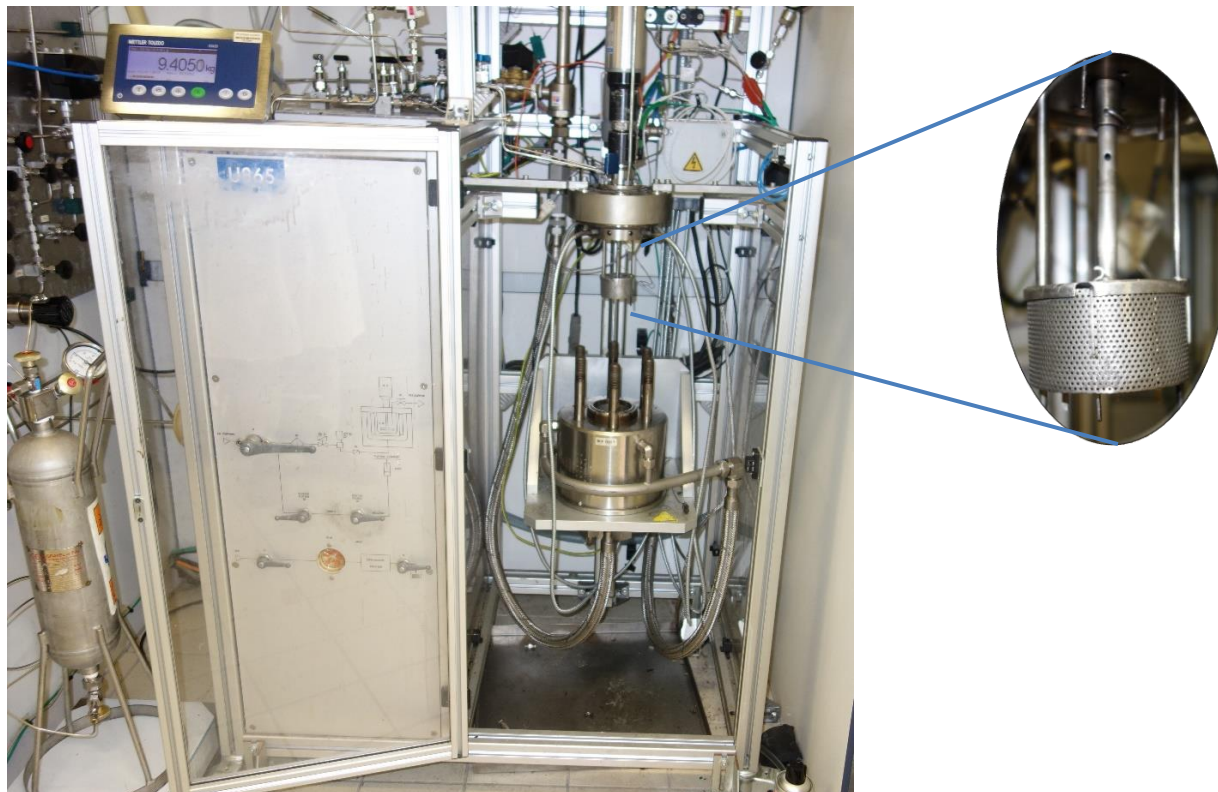


*Figure 3.2 - Photography of the U865 unit with zoom on the catalytic basket.*

The reactor is a batch type reactor with a volume of 550 cm<sup>3</sup>. There is a heating and a refrigerator jacket system surrounding the vessel of the reactor in order to operate at the desired temperatures; however, the refrigerator system uses air as a cooling fluid which is not very powerful. Connected to the reactor there are two inlet lines and two outlet lines. One inlet comes directly from the C<sub>3</sub> feed and the other one from the hydrogen/nitrogen ballast. The outlets are used for emptying the reactor and for sampling the reactor mixture. The “sampling” outlet is dipped inside the liquid phase. There is also a safety valve, preventing the system from exploding in the case that the reactor’s pressure becomes too high.

On the top of the vessel laid a changeable seal that kept the vessel and the reactor’s head together and that was changed from time to time due to the wear caused by the pression, to keep both parts together. Inside the vessel there is an annular cylinder-shaped basket of 165 cm<sup>3</sup> containing the catalyst. The impeller is adjusted in the center of the basket, and is pierced through, so that with high speed rotation, the pressure drop carries out the swallowing of the gas phase and the re-injection as small bubbles in the liquid phase. More information about the catalyst basket can be found in Braga (2015).

The basket is at such a level that allows all the catalyst particles to be immersed in the C<sub>3</sub> liquid phase during the whole experiment, and for every set of operating conditions utilized. It was noticed that sometimes, during the experimental run, some catalyst particles were able to leave the basket and fall on the bottom of the vessel, which is undesirable because those particles would be farther from the hydrogen source, but also would be thinner and thus possibly more active (less transport limitation). In order to avoid this event, two metal wires were wrapped in two opposite sides of the basket keeping it well closed during the experiment, which proved to be a successful implanted measure.

The C<sub>3</sub> bottle (Figure 3.3) used has a volume of 3.35 L and can be easily disconnected from the unit in order to be refilled with more industrial C<sub>3</sub> feed stored in a container located at IFPen reservoir zone. The bottle is placed over a balance in order to keep track of the amount of mass that is fed to the reactor. It has a barometer attached to it and, during the experimental part, the pressure in it ranges from 12.5 bar (after refill) to 10 bar. Below 10 bar there is not enough pressure to charge the reactor with the desired mass of C<sub>3</sub>, so it is necessary to fill it again.



Figure 3.3 - C<sub>3</sub> bottle and H<sub>2</sub>/N<sub>2</sub> ballast.



Figure 3.4 - Control panel of the U865.

A description of the hydrogen and nitrogen ballast can be found in the next section.

Next to the unit there is the control panel which is used to keep track and control some operating conditions such as the temperature, the pressure and the stirring speed of the impeller. The panel has a button system that is composed by: two buttons that control the general status of the unit (on and off buttons), two buttons that control the status of the

temperature regulation system (on and off buttons) and two buttons that control the status of the agitation (on and off buttons). For the agitation section there is also a turning manipulator that allows the selection of the impeller's speed of rotation. There are also a set of screens that indicate: the instantaneous temperature of the vessel's interior and the head of the reactor; the instantaneous pressure inside the vessel; and the instantaneous stirring speed of the impeller. Under both temperature screens there are some up and down buttons that allow to fix the set point for the temperature in those two zones, when the temperature regulation system is switched on. Besides all that, there is on top of the panel a screen that is constantly updated and shows the plot of all these indicators plus the ballast's pressure as a function of time. The control panel can be seen in Figure 3.4.

Despite the already existing system of pressure control, an extra barometer was added to the reactor with more precision in order to read very low pressures when needed (between 0 and 12 bara). This barometer was used in the procedure of emptying the reactor with a vacuum pump and also in the procedure of preparing a ballast composition with a low hydrogen partial pressure. The unit is directly connected to the nitrogen and hydrogen network of the site, which is at 200 bar.

#### **3.1.4 H<sub>2</sub>/N<sub>2</sub> Ballast**

The ballast used, with a volume of 0.6L, is fixed to the wall and it works as a reservoir for the hydrogen and nitrogen mixture that is used during an experimental run. The ballast can be seen in Figure 3.3 next to the grayel bottle. Right before the ballast there is a set of two valves that allows the sampling of the ballast mixture and also, via the addition of a precise barometer, allows to read the low amounts of hydrogen introduced in the ballast. More details about this protocol can be found in the Procedure section. After the ballast there is a combination of a regulating valve and a barometer that permit to choose and control the outlet pressure of the ballast that is fed into the reactor. After this system, there is an on/off safety valve that can cut the feeding of the reactor at any time in a quick way. This valve is also important in the task of keeping the desired pressure inside the reactor during the run.

Due to the unexpected decrease of the ballast's pressure in some set of experiments, gas leaks from the system were searched. In fact, with the use of a portable hydrogen detector it was possible to detect several micro-leaks and sometimes leaks near the valves connecting the gas network to the ballast, and there were also found some in the valves right after the ballast. In order to minimize the problem, a valve between the gas network and the ballast was replaced. However, despite it might have helped to fix the problem, there were still some concerning losses of pressure around the ballast. A severe review of the state of the connecting pipes and the valves is highly recommend before any more manipulations in this unit.

### 3.1.5 Procedure

This section is divided in the four major experimental tasks that were carried out: the leak test of the reactor, the catalyst pre-treatment, the operating of hydrogenation itself and the different processes of sampling that were adopted.

#### 3.1.5.1 Leak Test

The vessel was placed inside the unit with the seal on top of it. Every time at this point, it was checked if the seal smoothly slipped on the top of the vessel. If not, a better cleaning of the vessel and/or of the seal was needed. Then the basket was connected to the head of the reactor, and the bottom part of the unit was carefully elevated with an automatic lift. In order to keep the reactor at that position during the whole experiment, a set of six screws were tightened with the use of a dynamometric key. This adjustable tool allowed an incremental increase of the torque that those screws were tight, which lead to a more effective and correct sealing of the reactor. The screws were closed first at 70 N·m, then at 100 N·m and finally at 130 N·m. However, in the last set of experiments (from test 7 onwards) an even higher torque was necessary to keep it well sealed, so the reactor was closed with 150 N·m, achieved also with an incremental increase of the used torque.

The following steps are a part of the leak test. This test has a major importance in the context of the experimental work, because it will give the information if the reactor is correctly sealed or not. In the eventuality that it is not the case, during the experiment, a pressure drop would be seen due to the gas' leaks, and that could be misleading in the data treatment section.

At first, the nitrogen network valve was opened in order to clean the existing air that the vessel contained. This was a safety measurement, since the leak test was done with hydrogen, which is unsafe to put into contact with oxygen due to a risk of explosion. The reactor was cleaned three times with nitrogen, varying from 10 to 20 barg the reactor's pressure. Afterwards, the hydrogen network valve was opened and the reactor was cleaned three times with hydrogen following the same procedure. With the reactor empty again (containing approximately 1bara of hydrogen), it was filled again with hydrogen until reaching 50 to 60 barg. After letting the reactor's temperature and the pressure stabilize for about ten minutes, these two parameters are monitored regularly. The average pressure drop per hour is then calculated, and if this value is smaller than 0.6 bar/hour, the reactor is considered to be well sealed. This value was chosen instead of a lower one (0.3 bar/hour or even 0.2 bar/hour are commonly used in similar projects at IFPen) because in principle, there was not expected a substantial hydrogen consumption during the manipulations of this internship. Also, since during the experiments there was always a low percentage of hydrogen present inside the reactor, and being that the other compounds have all bigger molecules than hydrogen thus having more troubles in escaping

the reactor, the overall mass loss that would occur would be insignificant compared with the total mass of the system, if the 0.6 bar/hour were to be adopted as a decisive criterion.

In the eventuality that the reactor would not pass the leak test, the exit valve of the reactor was opened in order to let out all the hydrogen inside and after there were three options available. The lightest option that was adopted as the standard one before proceeding to more extreme measures was to re-tight the six screws with the dynamometric key at the same torque of 130 N·m. Then another leak test would be carried out using the protocol described before. If the result was still unsatisfactory, the reactor would be opened with the same key, and the seal would be changed for a new one, because it might be the case that the seal was too worn with the previously successive experiments, due to the pressures practiced. Nevertheless, and as already mentioned before, in the last set of experiments these measures were still not sufficient to keep the reactor well sealed so additional measures were needed. With the dynamometric key, the six screws were closed even tighter with a torque of 150 N·m, which proved to be effective as a last resource available. After discussing this method with laboratory technicians with recognized experience, they expressed that such an amount of torque was not normal in the U865 unit. They recommended that after the end of my experimental part with the unit, it should be dismantled and go for an extensive revision with a professional mechanic.

To conclude, one can trust all the executed experimental runs to have been performed without significant leakage events in the reactor section, but with probable leaks on the ballast section.

#### 3.1.5.2 Catalyst Pre-treatment

After ensuring that the reactor is properly sealed, it is necessary to activate the catalyst with a pretreatment. A temperature program is thus run with plateaus from 100 to 150 °C, under 10 to 20 barg.

#### 3.1.5.3 Manipulation

Normally, due to the long duration of the leak test and catalyst pre-treatment tasks, these two procedures took a whole working day to be completed. Only in the following day is it possible to finally prepare the manipulation and to execute it, taking its preparation one to one and a half hours and the manipulation itself took six hours for most of the experimental runs.

Primarily, the reactor is emptied by opening the exit valve letting out the hydrogen used for the catalyst's activation, remaining still inside approximately 1 bara of it. In order to eliminate this quantity that would induce an initial activity (before  $t_0$ ), and also to facilitate the sufficient amount of C<sub>3</sub> to be transferred to the reactor, a vacuum pump was used. A vacuum pump refrigerated with liquid nitrogen was connected to the reactor and the remaining hydrogen was aspirated. In Figure 3.5 the vacuum pump and the liquid nitrogen container can be seen.



Figure 3.5 - Vacuum pump and liquid nitrogen container.

Using a precise barometer that was not permanently connected to the reactor, the absolute pressure of the reactor was read and noted so that one can verify the efficiency of the hydrogen removal. After that, an almost non existing pressure is ensured (always below 0.02 bara), the reactor is again closed and the system of the vacuum pump is disconnected. Then, the bottom valve of the C<sub>3</sub> bottle is opened and the mass indicated in the balance is noted after waiting some time for its equilibrium to be reached. At this point, there is no C<sub>3</sub>-cut in the reactor since the reactor's entering valve is still closed which means that every C<sub>3</sub> that got out from the bottle is currently in the pipe between the C<sub>3</sub> bottle and the reactor. It is important that the measurement of the initial bottle's mass is done at this stage, since otherwise, a portion of the total C<sub>3</sub>-cut that went out from the bottle would not reach the reactor, thus having a lower quantity of C<sub>3</sub> than the one expected during the manipulation.

Later, the reactor's inlet valve is opened and the mass indicated in the balance is being monitored. When the subtraction of the actual mass indicated in the balance with the initial mass reaches the desired value of C<sub>3</sub>-cut to operate in the manipulation, the reactor's entering valve is closed. Then, the bottom valve of the C<sub>3</sub> bottle is also closed and the temperature regulation system is switched on with the desired operating temperature set.

While the reactor reaches the operating temperature, the gas mixture of the hydrogen and nitrogen ballast is prepared. For doing so, the gas mixture that was used in the previous manipulation is let out by opening the ballast's outlet valve that is connected to the general aspiration system of the laboratory. Since there will be some remains of the previous mixture, the ballast is purged three times with pure nitrogen gas from the network. To do so, the ballast's pressure is raised until 40 to 50 barg with nitrogen and then it is released to the aspiration system. Then the same precise barometer, fit for very low pressures and already used before, is connected to the top entry of the ballast and the pressure of the existing residues of nitrogen is measured and noted, which was always approximately 0.99 bara. Before

disconnecting this barometer from the system, the immediately preceding valve is closed so that no air enters in the system upon the removal.

Afterwards the objective is to introduce a very small and precise amount of hydrogen in the ballast to be used in the manipulation. For doing that, the upstream common lines of nitrogen and hydrogen relative to the ballast were all purged three times with pure hydrogen without any of it going to the ballast, as a result of the ballast's entering valve being closed. Then, the outlet pressure of the network's hydrogen gas was set to a minimum amount of 10 to 20 barg and resorting two consecutive valves close to each other, the hydrogen gas was carefully introduced in the ballast, using a precise barometer that is able to detect a minimum pressure of 0.001 bara. The two valve-trick consists in opening the first valve and letting the gas flowing until the second one that is closed at this point. Then the first valve is closed, stopping the gas flowing from the network, and there is at the time a small length pipe with pure H<sub>2</sub> inside of it with the same network's pressure. The second valve is a needle valve and it is slowly opened allowing a good control of a small input amount of H<sub>2</sub> into the ballast. At this point there is a mixture of the remaining traces of nitrogen used in the purge and the low amount of hydrogen just introduced. However, the hydrogen is still the most abundant component inside the ballast, and in this project one of the required operating conditions is to manipulate with excessively low concentrations of hydrogen (even reaching 0.5% of hydrogen). For this purpose, the upstream common lines of nitrogen and hydrogen relative to the ballast were all purged three times with pure nitrogen without any of it going to the ballast, as similarly done before. Then the outlet pressure of the network's nitrogen gas was raised to an amount higher than 100 barg and the ballast was fed with it until reaching a pressure close to 100 barg.

When the reactor, filled with the C<sub>3</sub>-cut, has reached thermal equilibrium at the desired temperature, the gas mixture of hydrogen and nitrogen is then added in order to reach the desired operating pressure. The outlet ballast valve is opened and at the downstream side there is one set of a regulating valve with a barometer that allows to choose the gas pressure that is fed into the reactor. By regulating it to a pressure slightly higher than the desired one inside the reactor, and by opening the reactor's inlet valve, the reactor is carefully filled with the gas mixture from the ballast. One should monitor constantly the reactor's pressure and temperature since this procedure is highly unstable due to: the transition of some of the C<sub>3</sub> from gas to the liquid phase, the increasing dissolution of hydrogen and nitrogen in the liquid phase, and the fact that the ballast's mixture that is being fed is at a lower temperature than the reactor's one.

In some experimental runs, this procedure was enough to start the manipulation, however for the set of experiments 9 to 12 it was decided that there would be a second ballast mixture being fed during the manipulation, with a higher hydrogen concentration than the one used at

first place (initial ballast). For doing so, after the initial ballast content is fed to the reactor, the ballast is emptied and a new ballast mixture is prepared following the same protocol as described before.

Afterwards, the impeller's agitation is started and set to a value approximately of 550 rotations per minute. At the same time the chronometer is started and this moment will mark the "t<sub>0</sub>" time. During the manipulation, there might occur some sampling procedures that will be explained in the next chapter. After a previously decided amount of time for the current manipulation, the agitation system and the regulation temperature system are switched off. Then the feeding valve connecting the ballast and the reactor is closed and the outlet reactor's valve is opened in order to evacuate all the gas and liquid inside.

#### 3.1.5.4 Sampling

During and after the manipulation there are carried out some sampling procedures applied to: the reactor's mixture liquid phase, the hydrogen and nitrogen mixture in the ballast, the used catalyst, and the green oil collected in the end. The sample containers are divided in balloons and in flasks.

##### a) Balloons

The balloons used for sampling have a volume of 1 litre, are transparent and are used for sampling both the reactor's liquid phase and the hydrogen and nitrogen mixture inside the ballast. For the reactor's liquid phase, a balloon is connected to one of the reactor's outlet that is always immersed in the liquid phase since the level of the extracting pipe is low enough in the unit's arrangement. Before any samples are taken out, the reactor's pressure and temperature are read in the control panel and noted. Also, the valve connecting the ballast and the reactor is closed in order to be able to estimate the exact pressure drop that this procedure brings. Then, that outlet valve is opened and some of the reactor's content is released to the air that will be further aspirated by the ambient aspiration system of the unit. This will serve to purge the outlet line from possible residues from previous manipulations. Then the balloon is inserted in the outlet pipe and the valve is opened carefully in order to avoid the balloon's bursting, and the new reactor's pressure and temperature are read and noted. The study of this pressure drop during the process of sampling is important so that one can evaluate if the mass loss of the system was significant when compared to its total mass. On average, 1 bar is lost every time a balloon sample is taken out, which represents approximately 1% of the total mass inside the vessel. This pressure drop will be compensated only with the gas mixture coming from the ballast, and no more C<sub>3</sub>-cut is added. With some of the noted values of pressure, the pressure history inside the reactor was schematized in Figure 3.6.

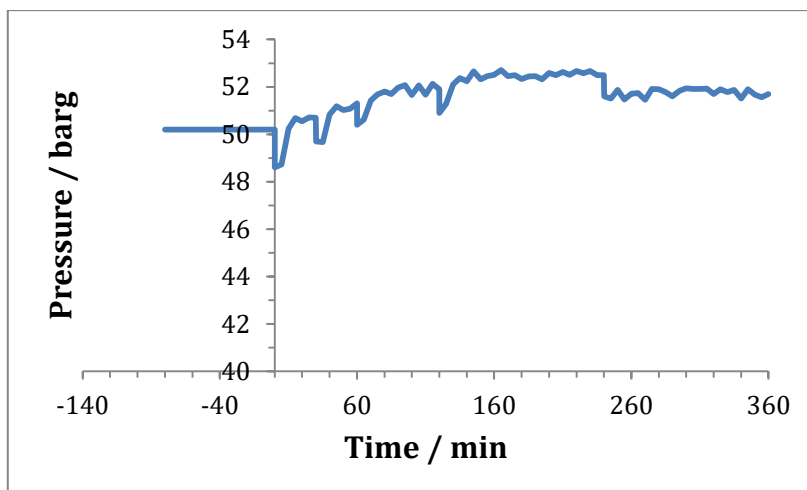


Figure 3.6 - Reactor's pressure history.

From this plot, the moments at which a sample is taken out can be clearly seen as pressure drops and can also be seen different set points of pressure from the beginning until the end of the run, which reveal minor limitations of the U865 unit concerning pressure control.

The ballast mixture is also sampled resorting to the use of a set of two consecutive valves on the top of the ballast and the outlet pipe is also purged before any sampling.

Initially, before all the experimental runs were executed, a study about the hydrogen leaks in the sampling balloons was made. The goal was to determine how much time is necessary in order for a significant amount of hydrogen to escape from the closed sampling balloon, leading to analysis with high analytical uncertainty. For doing so, a balloon was filled with a gas mixture of hydrogen plus nitrogen, and its hydrogen concentration was measured for several days in the gas chromatogram that is described in Section 3.2.2. The concentration of hydrogen as a function of time is plotted in Figure 3.7:

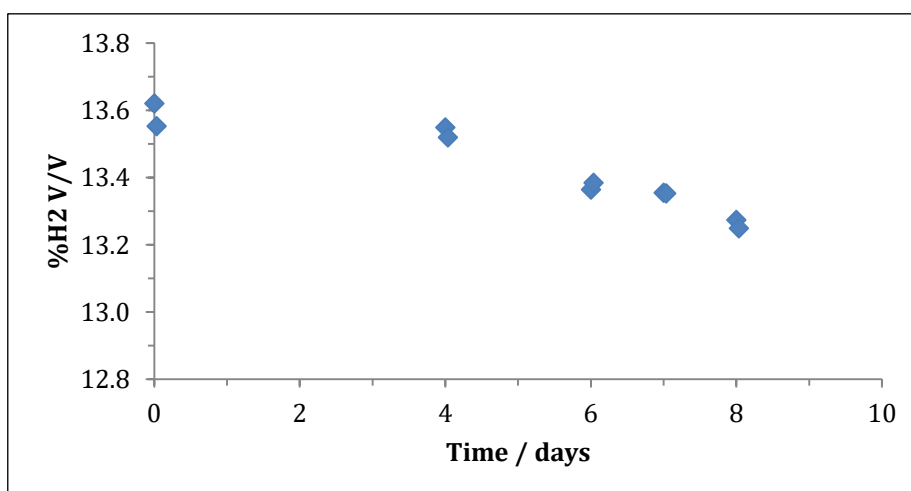


Figure 3.7 - Percentage of hydrogen in the balloon (v/v %) as a function of time.

From this study, one can conclude that the hydrogen content is stable enough (since it varies less than 0.5%) over 4 days after the sampling process is made. This study was important in order to be able to properly manage all the experimental tasks in the best way possible, without compromising the results obtained.

The samples injected on the GC analysors are taken from sampling balloons, at approximately standard temperature and pressure conditions (15 °C, 1atm). However the hydrocarbons inside can be heavy enough to not be totally vaporized in these conditions. In order to test this assumption, we ran thermodynamic calculations on the Proll v9.2 software, using either Soave-Redlich-Kwong (SRK) or Grayson-Streed (GS) equations. The list of considered molecules can be read on Table 3.2, and corresponds to C<sub>3</sub>-C<sub>9</sub> hydrocarbons that were available in the software, and still coherent with the nature of hydrocarbons that can be produced by oligomerization and oligo-cracking of MAPD.

Table 3.2 - List and concentration of the compounds used on the Proll.

Compound		Concentration %mol
<i>hydrogen</i>		10.0%
<i>propylene</i>	C <sub>3</sub>	65.0%
<i>propane</i>	C <sub>3</sub>	10.0%
<i>propadiene</i>	C <sub>3</sub>	3.0%
<i>methylacetylene</i>	C <sub>3</sub>	2.0%
<i>n-hexane</i>	C <sub>6</sub>	1.0%
<i>2,3-dimethyl-1,3-butadiene</i>	C <sub>6</sub>	1.0%
<i>cis-2-heptene</i>	C <sub>7</sub>	2.5%
<i>n-heptane</i>	C <sub>7</sub>	2.5%
<i>2,5-dimethyl-1,5-hexadiene</i>	C <sub>8</sub>	1.0%
<i>2,3-dimethyl-1-hexene</i>	C <sub>8</sub>	1.0%
<i>n-nonane</i>	C <sub>9</sub>	1.0%

In STP conditions, we could then observe that starting from C<sub>6</sub>-C<sub>7</sub>, less than half of the molecules are in liquid phase, and it needs 45 to 48 °C at atmospheric pressure to vaporize them all. This is illustrated in Figure 3.8.

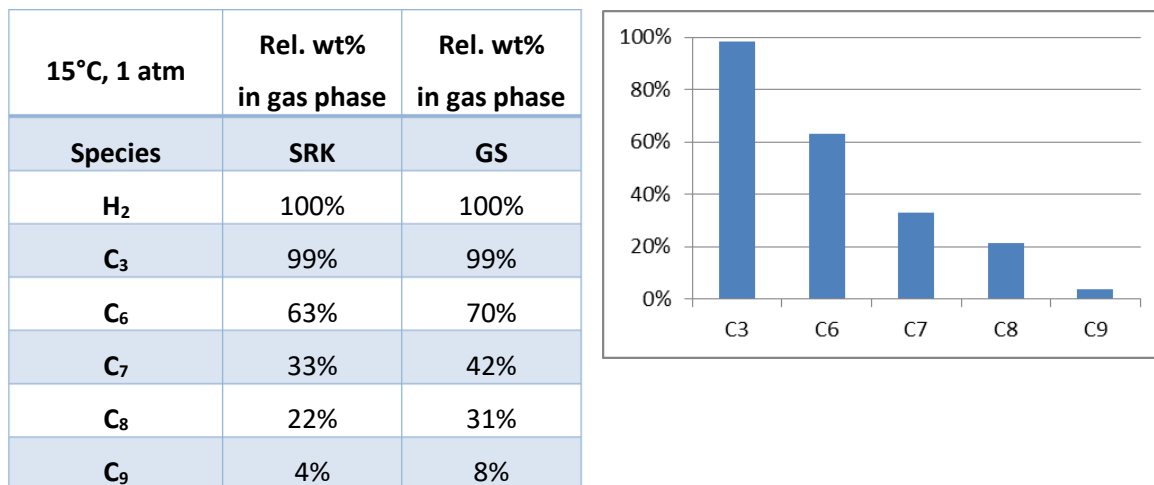


Figure 3.8 - Simulation results of SRK and GS models and the graphic representation of SRK.

From these simulations we can conclude that the amount of oligomers evaluated by GC analyses underestimates the amount inside the balloon by a factor of 1.5 to 5, depending on the volatility. It would be possible to correct the analyses at the condition that we can identify each molecule and affect it the right G/L repartition constant, however in our case, the oligomers are unknown. Then in this report we will keep the raw results of GC, while recalling that these amount are under-estimated.

#### b) Flasks

After the manipulation is done, the reactor is purged three times with nitrogen following the protocol already described before. Then the reactor is opened with the dynamometric key and the catalyst basket and the reactor's vessel are collected. The used catalyst is then gathered in an empty glass flask and stored for further analysis.

In order to collect the most of the green oil that is deposited on the bottom of the vessel, n-heptane is used as solvent to remove it, and then gathered in an empty glass flask. The total mass of the flask plus the green oil dissolved in n-heptane is weighted three times and the masses are noted with an uncertainty of 0.01g. The average masses of the flasks containing the green-oil dissolved in n-heptane can be found in Table 3.3:

Table 3.3 - Average masses for each test of the flask samples.

Test	Sample mass / g
1	20.13
2	19.03
3	19.44
4	19.68
5 & 6	20.57
7 & 8	20.81
9 & 10	20.47
11	19.43
12	20.43
13 & 14	20.51

The average mass of empty glass flasks was also evaluated on 26 elements, giving a mass average value of 18.02g and a standard deviation of 0.05g.

### 3.1.6 Operating Conditions

Before any manipulation or catalyst inclusion were done, the operating conditions to be tested were first tested on a simulator. In this simulator, several sets of operating conditions are simulated and the ones that would lead to satisfactory results are chosen to be reproduced in the U865 unit. The criteria used for evaluating the relevance of the simulated results are: a low hydrogenation of the MAPD (lower than 50%) since the reaction in study is the oligomerization and they are competitive reactions; a percentage of liquid C<sub>3</sub> inside the reactor higher than 50% since one must be sure that the catalyst is constantly fully wet; a good enough provision of hydrogen to the liquid phase in order to always maintain a slight H<sub>2</sub> coverage on the catalyst (which is referred as necessary for the oligomerization reaction to happen in the literature). The operating conditions studied can be found in Table 3.4:

Table 3.4 - Operating Conditions.

Test	P / barg	T / °C	Rpm	Catalyst mass / g	Uses of catalyst previously	HC mass / g	%H <sub>2</sub> ballast
1	25	23.5	1140	1.04	1	150.9	100.00%
2	40	30.0	570	0.49	1	164.3	2.41%
3	47	40.0	570	0.51	0	167.6	2.02%
4	52	50.0	510	0.51	0	176.6	2.31%
5	49	40.0	530	0.5	0	167.5	1.07%
6	47	40.0	530	0.5	1	148.1	1.08%
7	50	50.0	520	2	0	177.1	0.50%
8	49	50.0	550	2	1	171.3	0.50%
9	36-53	50.0	550	4.01	0	165.1	1.02% / 100.00%
10	51	50.0	560	4.01	1	175.4	0.50% / 11.07%
11	51	50.0	560	0.51	0	176,0	0.51% / 100.00%
12	50	50.0	520	2.01	0	169.7	0.58% / 100.00%
13	51	50.0	550	0.5	0	162.2	2.33%
14	51	50.0	540	0.5	1	169.1	2.35%

The first two manipulations were operated at the typical industrial hydrogenation process conditions, and had the intention to get acquainted with the unit, however only one of them was validated in the end. In the manipulation of test 9, there was such a quick decrease in the ballast's pressure that there was a point in which the ballast's pressure was not sufficient anymore to keep the reactor at 50 barg, so its pressure dropped to 36.4 barg.

## 3.2 Analysis

Four different analytical techniques were used in order to evaluate as much information as possible from the manipulations: two gas chromatograms with different columns, a thermogravimetric analysis (TGA) and a gas chromatography-mass spectrometry (GC-MS).

### 3.2.1 GC Alumina Bond ("GC AB")

#### 3.2.1.1 Specifications and Method

This gas chromatography setup has an alumina-bond type of column made by Restek (Rt-Alumina BOND/MAPD). Its specifications are listed in Table 3.5:

Table 3.5 - Specifications of the GC column,

Column material	Fused silica PLOT
Length / m	50
Internal Diameter / mm	0.32
Film thickness / $\mu\text{m}$	5

The injection procedure used for this column consists in extracting 2.5  $\mu\text{L}$  from the sample (balloon) with a gas syringe and then injecting that quantity manually in the GC's injector chamber. As for the GC's oven, its temperature profile chosen for enhancing the separation of compounds is represented in Figure 3.9.

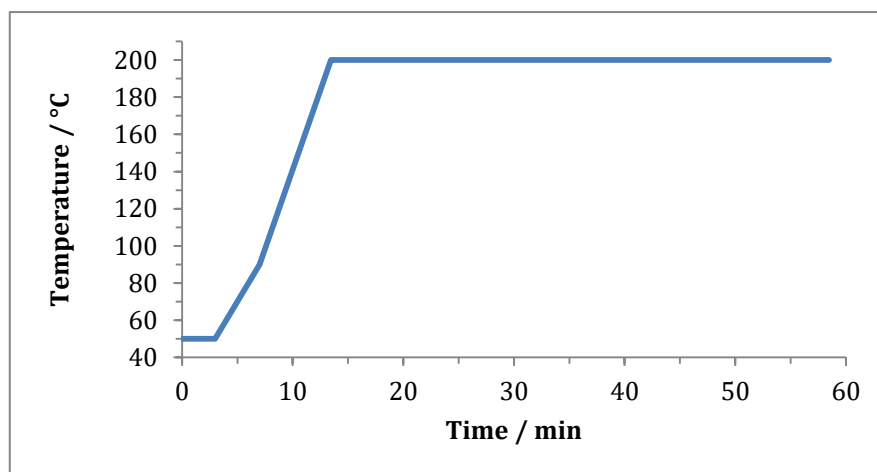


Figure 3.9 - GC's oven temperature history.

After the separation of the different compounds in the alumina column, the split ratio used is 1/100. The detector used for this analysis is one FID set at a temperature of 300°C. The carrier gas is pure helium with a 25 mL/min flowrate.

Due to analytical set up limitations, this chromatograph is only able to quantify hydrocarbons with a maximum of eight carbons. Thus, every oligomer identified with this method contains six to eight carbons (included).

### 3.2.1.2 Integration

The software automatically recognizes the peaks and integrates them. Every auto-integrated peak was then manually inspected and if the peak was not well integrated, it would be re-integrated manually. Regarding the software's integrator sensibility, the smallest peak area that it can detect was set at 1 pA, which for a C<sub>6</sub> compound equals to a concentration of  $2.74 \times 10^{-3}$  wt%. A coefficient of response was added to each compound in order to get a better

quantification of their concentrations. A table with those coefficients can be consulted in Table 3.6. For every oligomer the same coefficient of 1.075 was used.

Table 3.6 - Coefficient of response for the C<sub>2</sub> and C<sub>3</sub> compounds.

Compound	Coefficient of response
Ethane	1.150
Propane	1.125
Cyclopropane	1.125
Propylene	1.075
Propadiene	1.023
Propyne	1.030

Later, some C<sub>6</sub>, C<sub>7</sub> and C<sub>8</sub> compounds, with known chemical formula and concentration, were injected in the GC in order to have a better quantification of the oligomers' coefficient of response. The identified compounds are in the usual range of response factor: 0.75 to 1.25.

### 3.2.1.3 Reference Compounds (oligomers)

With the chromatograms obtained in this GC, two main regions were identified: the first one, well visible, where the ethane and the C<sub>3</sub> compounds can be quantified; and a later one, not well visible due to the low peak areas obtained, that allows the quantification of oligomers constituted by 8 carbons maximum. These two different zones can be found below in Figures 3.10 and 3.11:

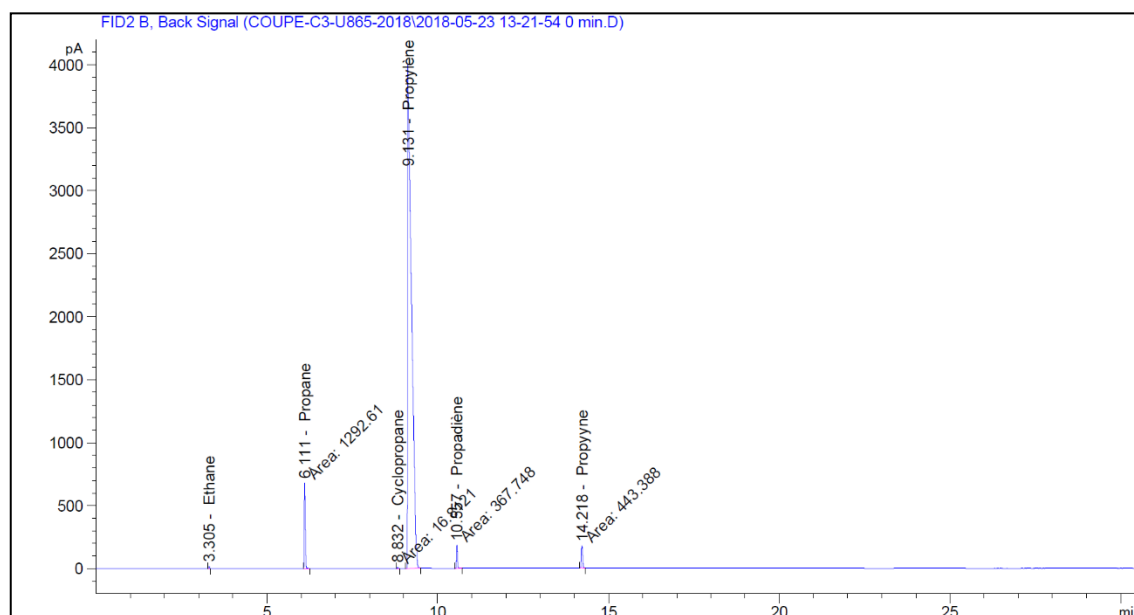


Figure 3.10 - Representative chromatogram of the GC AB without zoom.

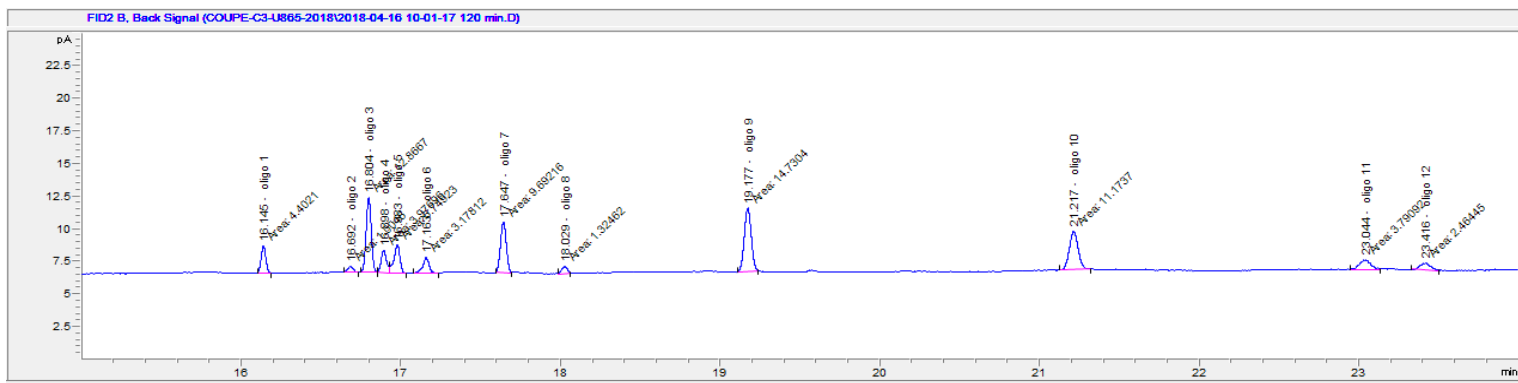


Figure 3.13 - Representative chromatogram of the GC AB with zoom.

For the first region (C<sub>2</sub> to C<sub>3</sub>), all peaks were already well identified by former projects, with the help of reference compounds. Concerning the unknown compounds of the second region, FID does not provide identification but only quantification, if a response coefficient is provided. For each unknown compound it was attributed the name of “oligo X” in which X varies from -2 to 13. Throughout the two months of tests, these compounds were tracked, despite the aging of the column, in order to build a coherent database. The shape of the produced peak curves and its resident time difference towards its neighbourhood peaks was also crucial in the process of identification. Every oligomer that was found in the GC is represented in the Figures 3.11 (oligo 1 to 12), 3.12 (oligo -2 to 0), 3.13 (oligo 13):

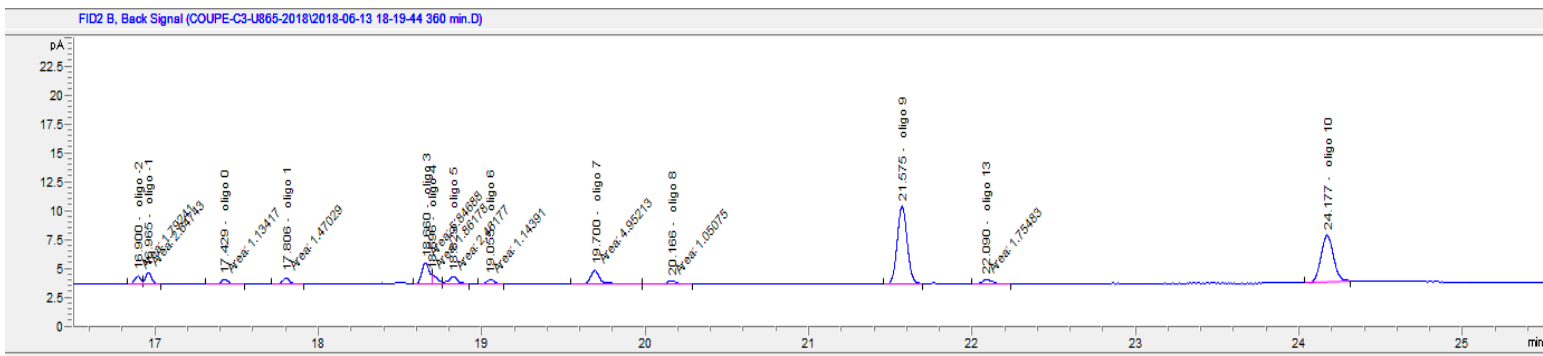


Figure 3.11 - Representative chromatogram of the GC AB with zoom.

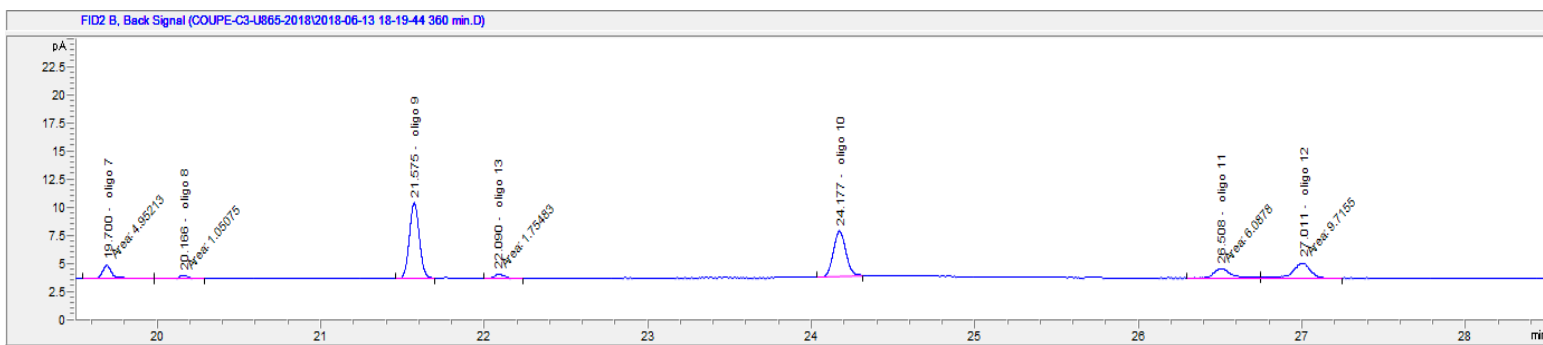


Figure 3.12 - Representative chromatogram of the GC AB with zoom.

With the constant use of this analytical method, the separating column started to show signs of aging such as: increase of the compounds' retention times and an increasingly worse separation of the nearest adjacent peaks. This shift varied between 38 seconds for the lightest compounds to 2 minutes and 42 seconds for the heaviest oligomers, for the last analysis.

### 3.2.2 GC used for estimating H<sub>2</sub> and N<sub>2</sub>

#### 3.2.2.1 Specifications and Method

This gas chromatograph has a system of 5 separating columns of 3 different types. A scheme of their disposition is illustrated in Figure 3.14:

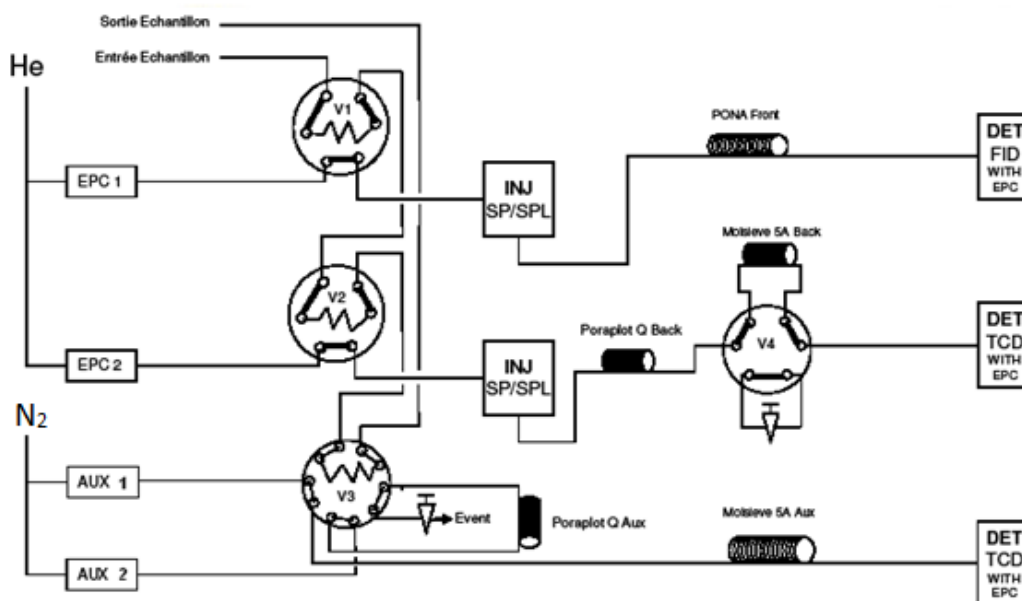


Figure 3.14 - Scheme of the GC used for estimating H<sub>2</sub> and N<sub>2</sub>.

The specifications about the 3 different types of column are listed in Table 3.7:

Table 3.7 - Specifications of the 3 column types used in the GC.

Stationary phase	PONA	HP-Plot Q	HP-Plot 5A
Length / m	50	30	30
Internal Diameter / mm	0.2	0.32	0.32
Film thickness / μm	0.5	20	1

The injection procedure used for this column consists in connecting the sampling balloon to the GC's injector by a thin metallic wire passing through a rotameter. Then the balloon is pressed during 20 seconds, filling a closed loop with 0.5 mL of sample which is injected afterwards in the GC. The temperature profile chosen for enhancing the separation of compounds is represented in Figure 3.15:

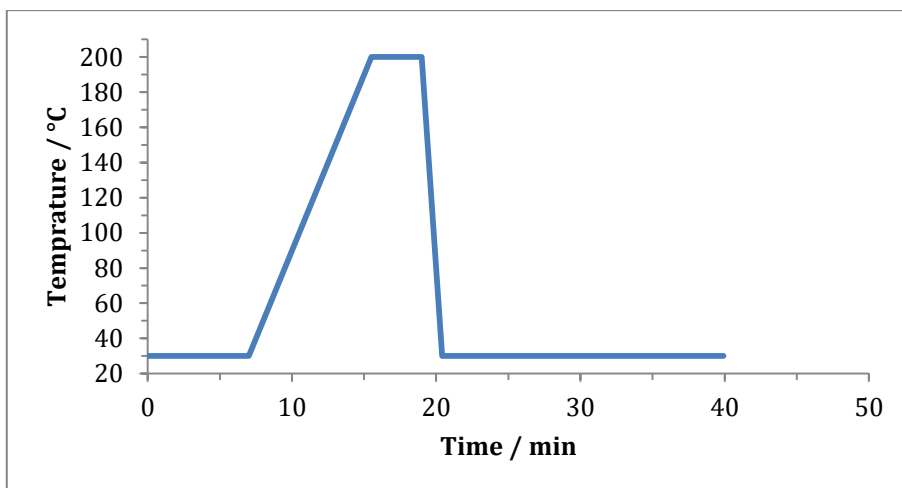


Figure 3.15 - GC's oven temperature history.

For this analysis three different detectors are used: one FID detector (FID1 A) and two TCD detectors (TCD2 B and TCD3 C). The temperature of the detectors is 250°C. The carrier gas is helium for the FID detector and TCD2 B with a flowrate of 8 mL/min, whereas for the TCD3 C it is nitrogen with a flowrate of 8.2 mL/min. With this analytical tool, the concentration of H<sub>2</sub>, N<sub>2</sub> and the overall C<sub>3</sub>-cut concentration can be quantified. In Figure 3.16 one example of chromatogram is presented.

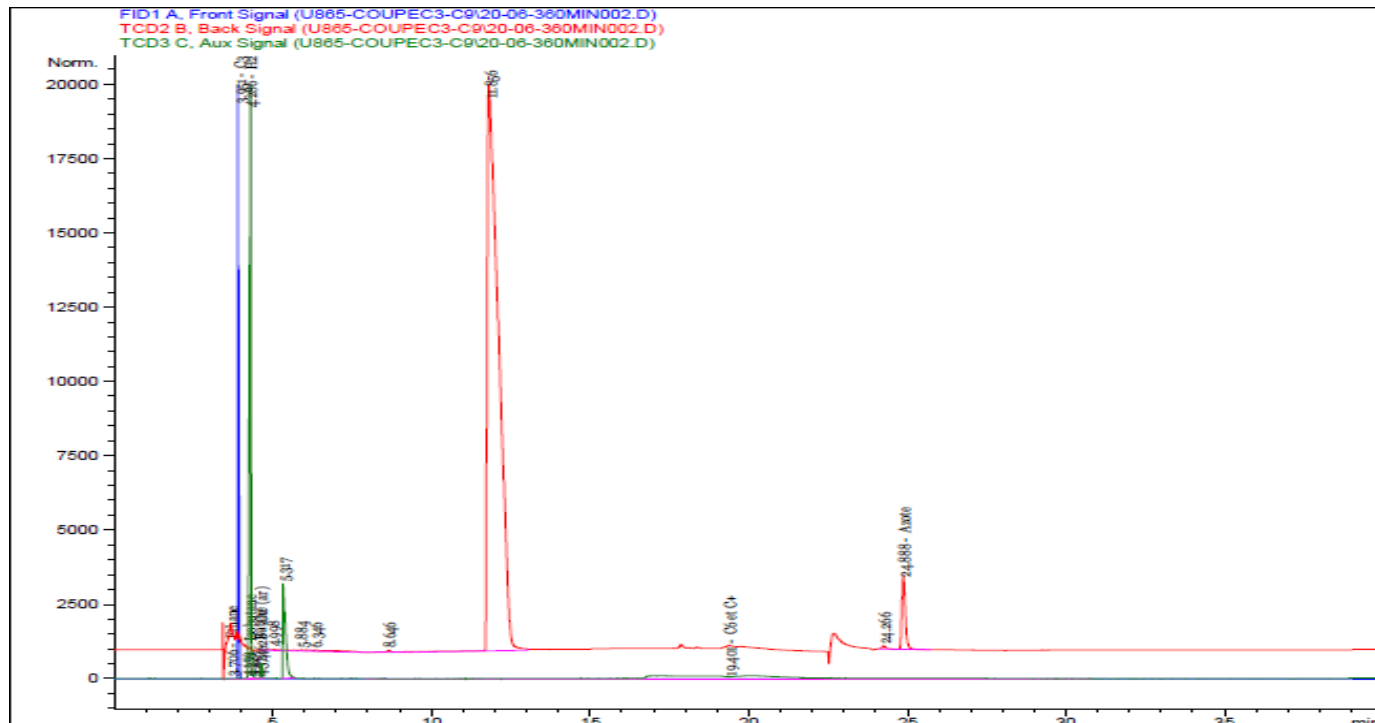


Figure 3.16 - Representative chromatogram of the GC used for estimating H<sub>2</sub> and N<sub>2</sub>.

## 3.2.2.2 Integration

For the integration of the obtained peaks, the same procedure as described in section 3.1.2 was applied. For this chromatogram, the minimum amount of area detectable is 1 pA, which corresponds to a minimum concentration of  $1.16 \times 10^{-3}$  wt% for H<sub>2</sub> and  $1.01 \times 10^{-2}$  wt% for N<sub>2</sub>. The response coefficients are available on the Table 3.8 below.

*Table 3.8 - Coefficient of response used for each compound.*

Compound	Coefficient of response
C <sub>3</sub> -cut	$2.69 \times 10^{-3}$
Hydrogen	$1.16 \times 10^{-3}$
Nitrogen	$1.01 \times 10^{-2}$

## 3.2.2.3 Calibration

Since this device should be calibrated every year and in the present year no calibration was already done, a new calibration was performed. For doing so, two different standards of known composition, made by Air Liquide, were injected and the areas obtained in the chromatograms were measured. The composition of each gas mixture is described in Table 3.9:

*Table 3.9 - Composition of the calibrating gas bottles.*

	Bottle 1	Bottle 2
Compound	V/V %	V/V %
H <sub>2</sub>	76	1
CO	2	5
N <sub>2</sub>	2	85.5
O <sub>2</sub>	0	1
CO <sub>2</sub>	2	5
CH <sub>4</sub>	10	0.5
C <sub>2</sub> H <sub>6</sub>	2	0.5
C <sub>3</sub> H <sub>8</sub>	2	0.5
C <sub>4</sub> H <sub>10</sub>	2	0.5
C <sub>5</sub> H <sub>12</sub>	2	0.5

After doing three analyses for each bottle and doing the average of the areas for each different compound, the response coefficients presented previously in Table 3.8 for light gases and alkanes were obtained.

### 3.2.3 Thermogravimetric Analysis (TGA)

In this analysis, a sample of the collected catalyst is crushed into powder and its mass is monitored as a function of time as the sample specimen is subjected to a controlled temperature program in a controlled atmosphere. The temperature program chosen is represented in Figure 3.17.

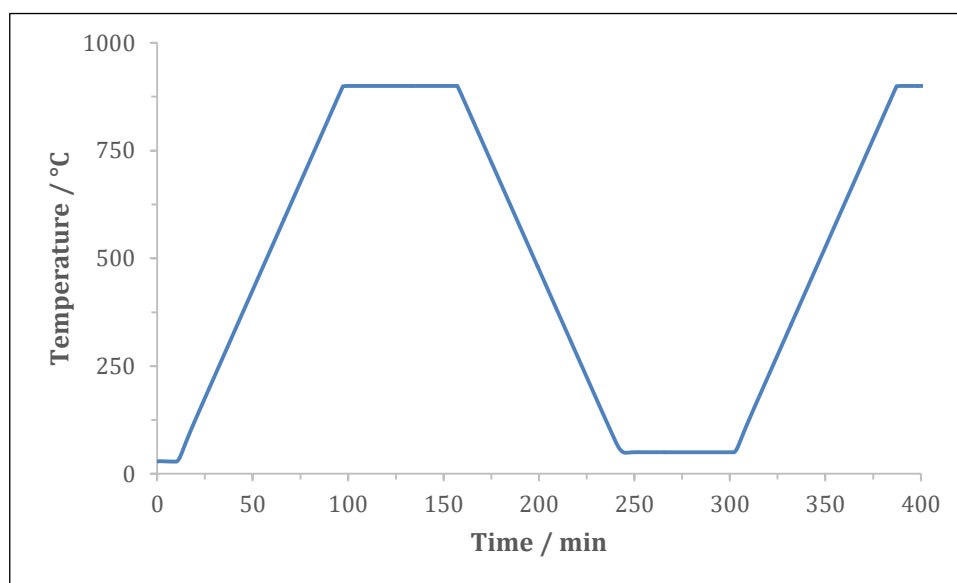


Figure 3.17 - Oven's temperature history.

For the first ramp of temperature, the sample is submitted in an atmosphere of nitrogen (called “desorption cycle”), whereas for the second temperature ramp in an atmosphere of air (called “combustion cycle”). The loss of mass of the sample is plotted as a function of the run time. In Figure 3.18, one exemplary result can be found:

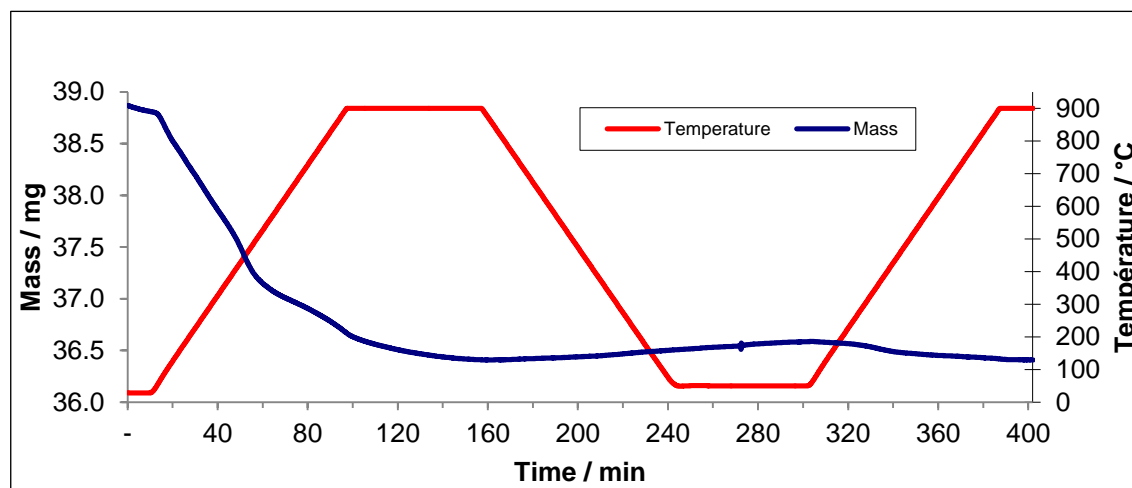


Figure 3.18 - Representative TGA results for test 1.

### 3.2.4 Gas Chromatography-Mass Spectrometry (GC-MS)

The GC-MS is composed of two major building blocks in series: the gas chromatograph and the mass spectrometer. Just like the previous gas chromatographs, it utilizes a capillary column which provides the separation of the molecules as the sample travels through the length of the column. The molecules are retained by the column and then leave the column at different retention times, allowing the mass spectrometer downstream to capture, ionize, accelerate, deflect, and detect the ionized molecules separately. In an “Electron Ionization (EI)” setup, the mass spectrometer does this by breaking each molecule into ionized fragments by bombarding it with electrons and detecting these fragments using their mass-to-charge ratio. The specifications of the GC column are listed in Table 3.10:

Table 3.10 - Specifications of the GC-MS column.

Column material	PONA
Length / m	50
Internal Diameter / mm	0.2
Film thickness / $\mu\text{m}$	0.5

The temperature profile of the oven utilized in the gas chromatograph is represented in Figure 3.19:

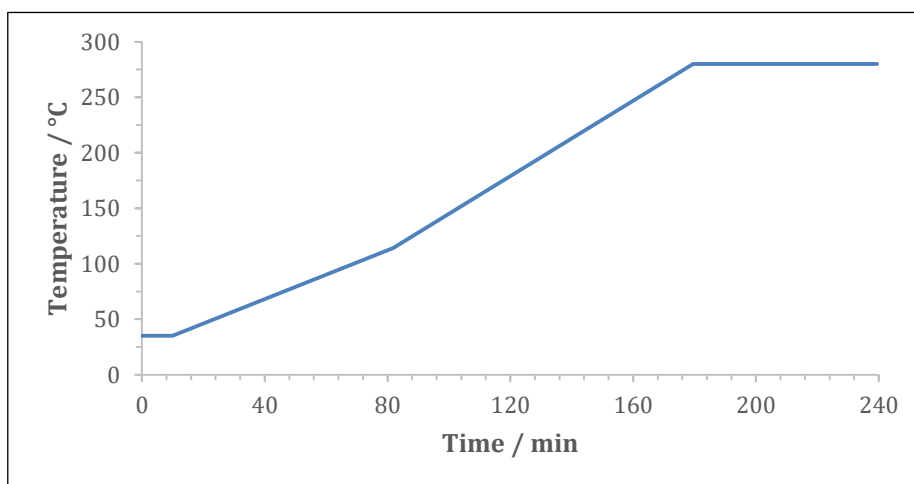


Figure 3.19 - Oven's temperature history.

The injection volume of Green Oil was constant and fixed to a value of 0.5  $\mu\text{L}$ , the temperature of the injector was set at 280°C (to make sure every oligomers were evaporated). For this analysis the carrier gas was helium and a split rate of 100 was applied. No graph of this method will be presented, only the direct results obtained by them.

## 4 Results

### 4.1 Mass balance: how to consider it for oligomers

Recapping, there will be 3 types of different sampling procedures that will give us information from three different sources of oligomers inside the reactor. During the manipulation, there are the sampling balloons that will provide the information about the oligomer content inside the reactor's liquid phase, but only until oligomers containing 8 carbons. Also, since there is the condensation of some oligomers inside the balloon, only the gas fraction inside the balloon can be measured (cf. §3.1.5.4). At this time, the oligomers that are “trapped” inside the catalyst cannot be quantified. After the test, there are the flasks containing the collected green oil and the collected catalyst unwashed, while the lighter oligomers were evacuated with the rest of the reactor's inside content. The green oil will provide the information about the content of the heavier oligomers that were produced in that manipulation. The collected catalyst will provide information about the oligomers that were formed in the manipulation and that didn't get out of it during the manipulation (by washing) and during the purging procedure with N<sub>2</sub>. In Figure 4.1 is a representative scheme of the repartition of oligomers and the available analyses:

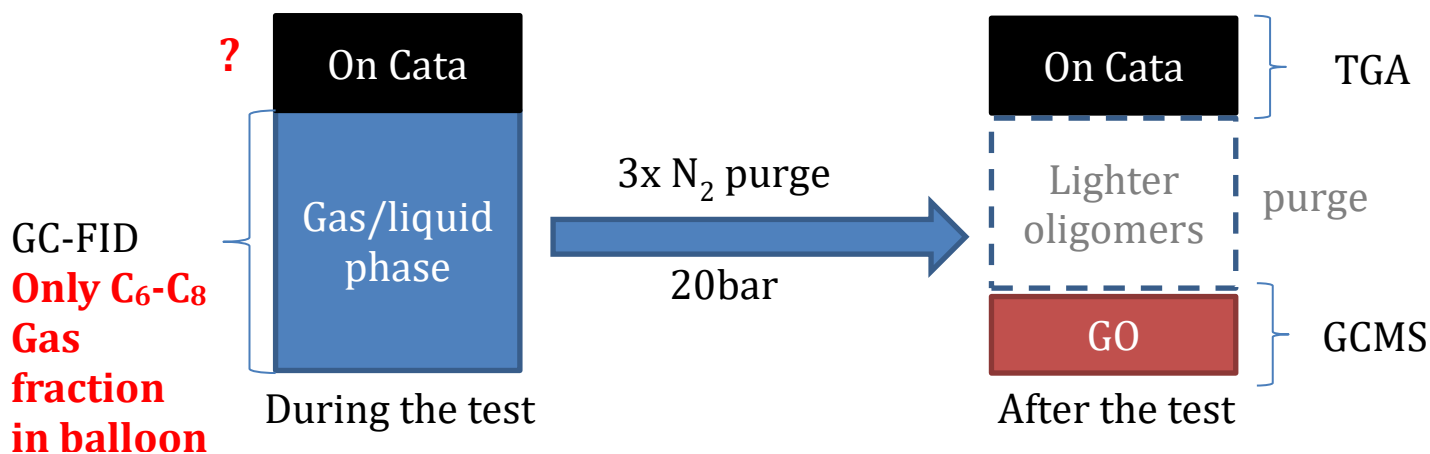


Figure 4.1 - Scheme of the repartition of oligomers and how to analyse them.

However, since the catalyst when collected is not washed, one can make the assumption that the amount of heavy oligomers inside the catalyst during the test is approximately the same than the one after the test, thus it can be evaluated by TGA.

The results obtained during the different tests are presented in the next sections. There are 14 validated tests and in the cases where the catalyst was not replaced from one manipulation to another, the two tests are grouped and their results are presented together. For every test, the data gathered from the two gas chromatograms is presented in one single table, being the

detailed data of C<sub>3</sub>-C<sub>8</sub> molecules from the “GC AB” with the “total C<sub>3</sub>” rescaled to the data of the GC used for estimating the H<sub>2</sub> and N<sub>2</sub>.

In the end, 16 different oligomers from C<sub>6</sub> to C<sub>8</sub> are reported and are divided in 5 different populations:

- The hydrogenated oligomers, oligo -2 and oligo -1
- The lighter oligomers, from oligo 3 to oligo 7;
- The medium oligomers, oligo 9 and oligo 10;
- The heavier oligomers, oligo 11 and oligo 12;
- The rest, consisting in oligo 0, oligo 1, oligo 2, oligo 8 and oligo 13.

The nomenclature used for identifying the oligomers was already described in the subchapter §3.2.1.3. In order to decide in which populations the oligomers should be divided in, the change of concentration for each oligomer with the change of the operating conditions was analyzed, and if it is significant enough and if other oligomers behave the same way, they were grouped in one population.

For each test the oligomer concentration is shown and it is important to remember that with the GC method, only oligomers containing from six to eight carbons can be quantified. All the complete GC tables can be consulted in Appendix 1. It's important to refer that in the cases where the tests show less samples it's due to the fact that the others analyses of the samples were not validated.

## 4.2 Test 1 - standard hydrogenation conditions

For this test exceptionally, instead of trying to maximize the oligomerization reaction, a typical hydrogenation reaction was carried out in its classic conditions. The operational conditions that were carried out in this test can be found in Table 4.1:

*Table 4.1 - Operating conditions of test 1.*

Test	P / barg	T / °C	rpm	Catalyst mass / g	# uses catalyst before	HC mass / g	%H <sub>2</sub> ballast
1	25.0	23.5	1140	1.04	1	150.9	100.00%

For this test, the history of concentration for each oligomer population was plotted as a function of time in Figure 4.2:

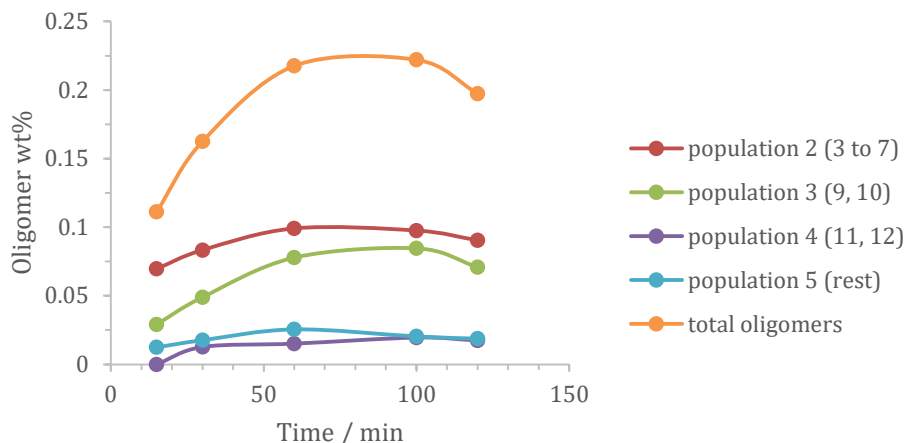


Figure 4.2 - Test 1 populations's history.

The results obtained for quantifying the oligomer formation are summarized in Table 4.2:

Table 4.2 - Obtained results in GC AB, TGA and GC-MS for test 1.

GC AB		TGA		GC-MS	
oligomer wt%	0.20	desorbed mass	4.8%	oligomer wt%	3.71
<b>oligomer mass / mg</b>	<b>297.98</b>	<b>oligomer mass / mg</b>	<b>52.59</b>	sample mass / g	2.11
		combusted mass	0.3%	<b>oligomer mass / mg</b>	<b>78.38</b>
		<b>coke mass / mg</b>	<b>3.13</b>		

### 4.3 Test 2

After simulating several different operating conditions, these were the ones to be first chosen to try to minimize the hydrogenation, while hopefully maximizing the oligomer production (Table 4.3):

Table 4.3 - Operating conditions of test 2.

Test	P / barg	T / °C	rpm	Catalyst mass / g	# uses catalyst before	HC mass / g	%H <sub>2</sub> ballast
<b>2</b>	40.0	30.0	570	0.49	1	164.3	2.41%

From the hydrogenation conditions (run 1), the catalyst mass was cut to half, while the temperature was increased in order to achieve higher catalyst activity. The number of rotations per minute of the impeller was significantly decreased to a point where there might be mass transfer limitations, and also low enough in order to reduce the washing of the catalyst, as an attempt to produce even more oligomers. The hydrogen percentage was also decreased to an extremely low concentration, in order to reduce hydrogenation, but still without absence of it since the oligomerization seems to need the presence of a slight amount of hydrogen on the catalyst. The pressure was then adjusted in order to achieve the necessary conditions described

in chapter 2.6, especially guaranteeing that the C<sub>3</sub> is mainly in the liquid phase. For this test, the history of concentration for each oligomer population was plotted as a function of time in Figure 4.3:

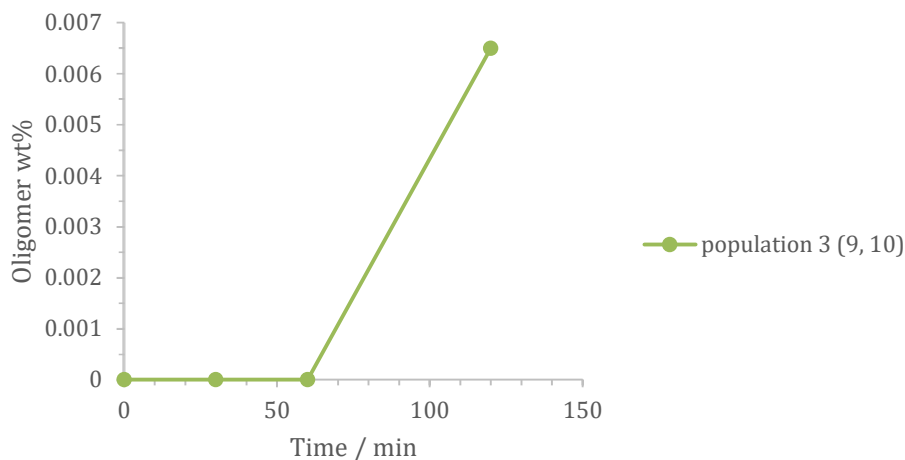


Figure 4.3 - Test 2 populations' history.

The results obtained for quantifying the oligomer formation are summarized in Table 4.4:

Table 4.4 - Obtained results in GC AB, TGA and GC-MS for test 2.

GC AB		TGA		GC-MS	
oligomer wt%	$6.50 \times 10^{-3}$	desorbed mass	4.0%	oligomer wt%	0.19
<b>oligomer mass / mg</b>	<b>10.69</b>	<b>oligomer mass / mg</b>	<b>20.54</b>	sample mass / g	1.01
		combusted mass	0.6%	<b>oligomer mass / mg</b>	<b>1.97</b>
		<b>coke mass / mg</b>	<b>2.96</b>		

#### 4.4 Test 3

The operational conditions that were carried out in this test can be found in Table 4.5:

Table 4.5 - Operating conditions of test 3.

Test	P / barg	T / °C	rpm	Catalyst mass / g	# uses catalyst before	HC mass / g	%H <sub>2</sub> ballast
<b>3</b>	47.0	40.0	570	0.51	0	167.6	2.02%

Comparing with the previous run, in this one the temperature was increased from 30°C to 40°C in order to obtain a higher catalyst activity. The pressure was also increased since the oligomerization reaction order is higher than the hydrogenation reaction order, thus increasing the pressure will promote the oligomerization over hydrogenation. Despite trying to have the same hydrogen concentration in the ballast as before, its concentration dropped to 0.39%. Due to the difficulties in the pressure control of the unit, the average pressure during the test was

47.0 barg instead of the desired 50.0 barg. For this test, the history of concentration for each oligomer population was plotted as a function of time in Figure 4.4:

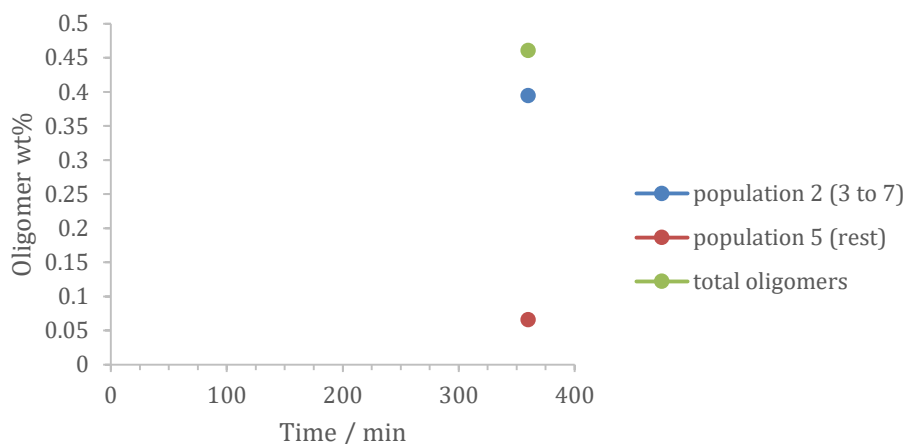


Figure 4.4 - Test 3 populations' history.

The results obtained for quantifying the oligomer formation are summarized in Table 4.6:

Table 4.6 - Obtained results in GC AB, TGA and GC-MS for test 3.

GC AB		TGA		GC-MS	
oligomer wt%	0.46	desorbed mass	4.5%	oligomer wt%	0.02
<b>oligomer mass / mg</b>	<b>772.67</b>	<b>oligomer mass / mg</b>	<b>24.18</b>	sample mass / g	1.42
		combusted mass	0.6%	<b>oligomer mass / mg</b>	<b>0.21</b>
		<b>coke mass / mg</b>	<b>3.08</b>		

## 4.5 Test 4

Before starting this new test, one of the valves connecting the ballast to the gas network was replaced due to the poorly sealing in the pipe when the valve was fully closed. The operating conditions that were carried out in this test can be found in Table 4.7:

Table 4.7 - Operating conditions of test 4.

Test	P / barg	T / °C	rpm	Catalyst mass / g	# uses catalyst before	HC mass / g	%H <sub>2</sub> ballast
4	52.0	50.0	510	0.51	0	176.6	2.31%

Comparing with the previous run, in this one the temperature was increased from 40 °C to 50 °C in order to obtain an even higher catalyst activity. For this test, the history of concentration for each oligomer population was plotted as a function of time in Figure 4.5:

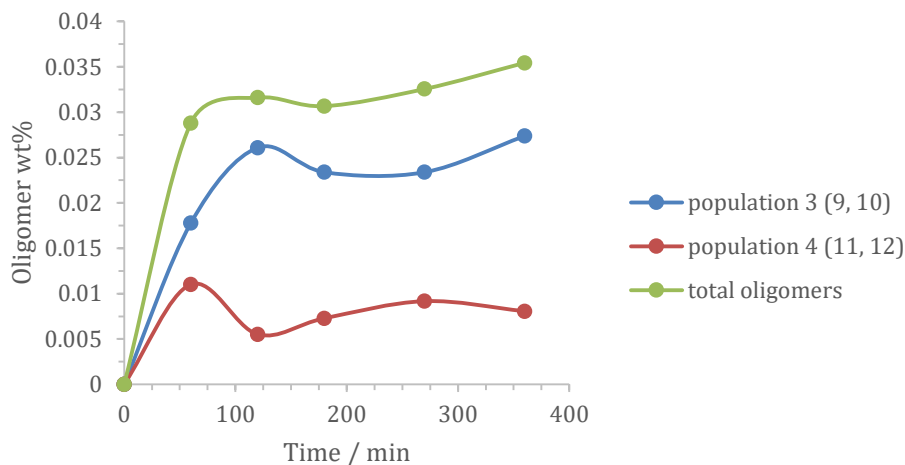


Figure 4.5 - Test 4 populations' history.

The results obtained for quantifying the oligomer formation are summarized in Table 4.8:

Table 4.8 - Obtained results in GC AB, TGA and GC-MS for test 4.

GC AB		TGA		GC-MS	
oligomer wt%	$3.54 \times 10^{-2}$	desorbed mass	5.8%	oligomer wt%	0.04
<b>oligomer mass / mg</b>	<b>62.59</b>	<b>oligomer mass / mg</b>	<b>31.53</b>	sample mass / g	1.66
		combusted mass	0.4%	<b>oligomer mass / mg</b>	<b>0.66</b>
		<b>coke mass / mg</b>	<b>2.05</b>		

## 4.6 Tests 5 and 6

These were the first two consecutive tests that were successfully both validated. The objective of executing each set of operating conditions in pairs of tests is that after the second test, the amount of green oil recovered would be bigger, and thus easier to detect in the GC-MS. The green oil is only recovered after the second test and never immediately after the first test. The operating conditions that were carried out in these tests can be found in Table 4.9:

Table 4.9 - Operating conditions of tests 5 and 6.

Test	P / barg	T / °C	rpm	Catalyst mass / g	# uses catalyst before	HC mass / g	%H <sub>2</sub> ballast
5	49,0	40,0	530	0.50	0	167.5	1.07%
6	47,0	40,0	530	0.50	1	148.1	1.08%

In this pair of runs, the main operating condition that was changed relatively to the other tests was the hydrogen concentration in the ballast that was cut in half. For these tests, the history of concentration for each oligomer population was plotted as a function of time in Figure 4.6:

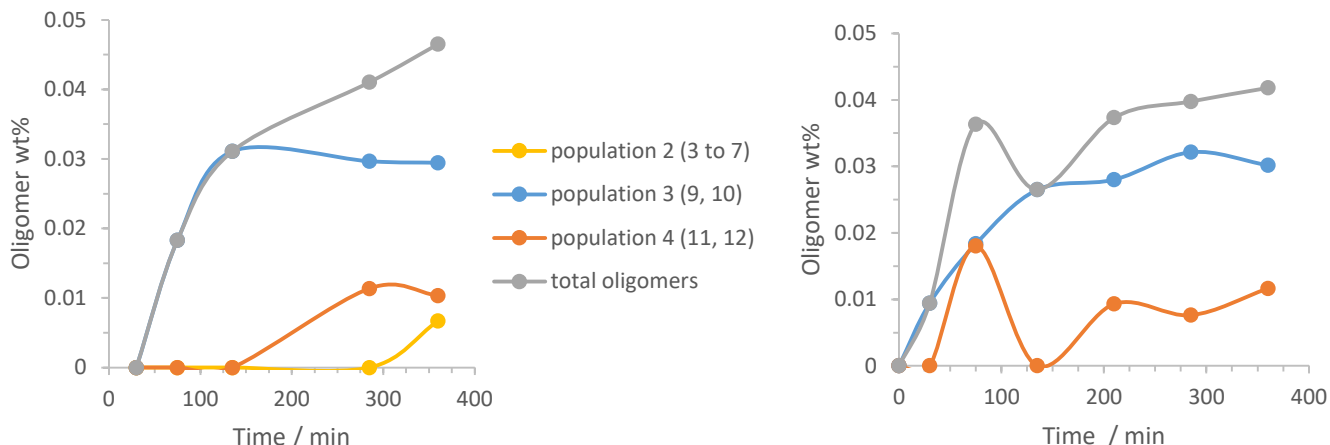


Figure 4.6 - Test 5 (left) and test 6 (right) population's history.

The results obtained for quantifying the oligomer formation are summarized in Table 4.10 and 4.11:

Table 4.10 - Obtained results in GC AB for tests 5 and 6.

GC AB Test 5		GC AB Test 6	
oligomer wt%	$4.65 \times 10^{-2}$	oligomer wt%	$4.18 \times 10^{-2}$
oligomer mass / mg	<b>77.90</b>	oligomer mass / mg	<b>61.91</b>

Table 4.11 - Obtained results in TGA and GC-MS for tests 5 and 6.

TGA		GC-MS	
desorbed mass	3.7%	oligomer wt%	0.86
<b>oligomer mass / mg</b>	<b>19.31</b>	sample mass / g	2.55
combusted mass	0.5%	<b>oligomer mass / mg</b>	<b>22.02</b>
<b>coke mass / mg</b>	<b>2.51</b>		

## 4.7 Tests 7 and 8

The operating conditions that were carried out in these tests can be found in Table 4.12:

Table 4.12 - Operating conditions for tests 7 and 8.

Test	P / barg	T / °C	rpm	Catalyst mass / g	# uses catalyst before	HC mass / g	%H <sub>2</sub> ballast
<b>7</b>	50,0	50,0	520	2.00	0	177.1	0.50%
<b>8</b>	49,0	50,0	550	2.00	1	171.3	0.50%

For this pair of tests, one of the two major changes in the operating conditions is the ballast composition. In these extreme conditions, only 0.5% (v/v) of the ballast mixture is hydrogen, being the rest nitrogen which was the lowest hydrogen concentration achieved during this

project. The other major change is that the mass of catalyst went from 0.50g to 2.00g. This increase has the purpose of simulating bigger batch times, i.e., by increasing the amount of catalyst available, these reactions will occur faster. For these tests, the history of concentration for each oligomer population was plotted as a function of time in Figure 4.7:

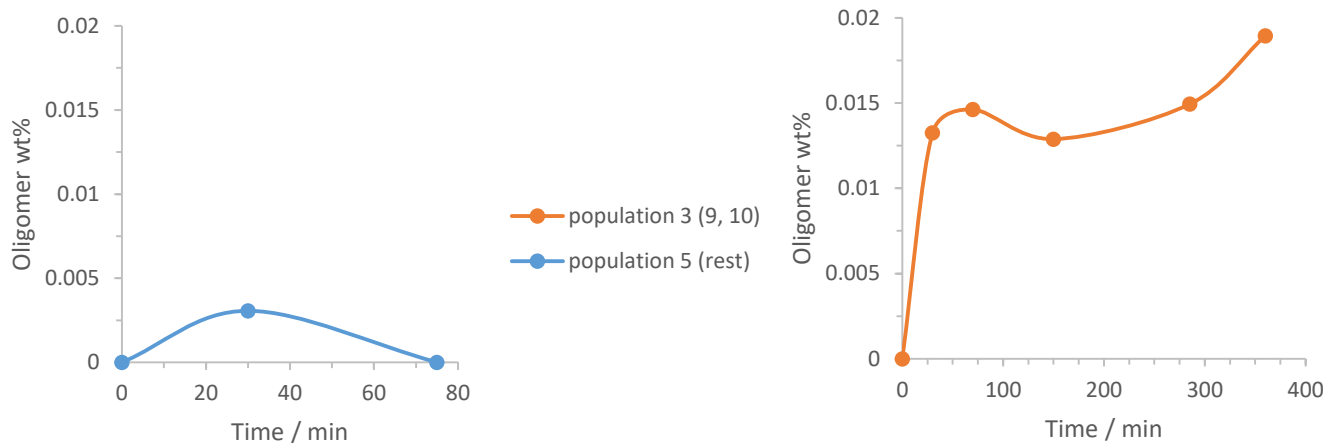


Figure 4.7 - Test 7 (left) and test 8 (right) populations' history.

In Appendix 2 it is possible to see a photography of the green-oil and the used catalyst collected in those tests. The results obtained for quantifying the oligomer formation are summarized in Tables 4.13 and 4.14:

Table 4.13 - Obtained results in GC AB for tests 7 and 8.

GC AB Test 7		GC AB Test 8	
oligomer wt%	0.00	oligomer wt%	$1.89 \times 10^{-2}$
oligomer mass / mg	0.00	oligomer mass / mg	32.44

Table 4.14 - Obtained results in TGA and GC-MS for tests 7 and 8.

TGA		GC-MS	
desorbed mass	2.3%	oligomer wt%	0.10
oligomer mass / mg	47.22	sample mass / g	2.86
combusted mass	0.3%	oligomer mass / mg	2.96
coke mass / mg	6.02		

## 4.8 Tests 9 and 10

The operating conditions that were carried out in these tests can be found in Table 4.15:

Table 4.15 - Operating conditions for tests 9 and 10.

Test	P / barg	T / °C	rpm	Catalyst mass / g	# uses catalyst before	HC mass / g	%H <sub>2</sub> ballast
9	36.0-53,0	50,0	550	4.01	0	165.1	1.02% / 100.00%
10	51,0	50,0	560	4.01	1	175.4	0.50% / 11.07%

After completing the tests 7 and 8, it was conjectured that a hydrogen percentage of 0.5% in the ballast might be too low for runs longer than one hour. Due to the fact that for each bar of hydrogen that is consumed, only 0.005 bar of hydrogen will be fed again into the reactor from the ballast, which leads to a completely absence of this gas over time. This conclusion will be better explained in chapter 5. Hence, in order to have a small presence of hydrogen along the 6 hours of running time, two ballasts with different compositions are prepared for one single test. The first (or initial) ballast with very low concentration of hydrogen will pressurize the reactor with the C<sub>3</sub>-cut, from its autogenic pressure until the desired operating pressure. And after, the second (or feeding) ballast that will have a higher concentration of hydrogen and will be fed into the reactor right after the agitation starts.

Following the same ideas of the tests 7 and 8, the mass of catalyst was doubled from 2.00g to 4.01g. However, the basket was filled with too many particles since, in the end of test 10, the reactor was opened and about 40% of the catalyst particles had left the catalytic basket and were deposited in the bottom of the vessel. This affects the manipulation since these bottom particles are not so exposed anymore to the hydrogen gas coming from the impeller.

During test 9, there was such a quick decrease in the ballast's pressure that there was a time in which the ballast's pressure was not sufficient anymore to keep the reactor at 50.0 barg, so its pressure dropped to 36.4 barg. After this event, the reactor's pressure was restored to 53.0 barg by adding pure hydrogen. Despite all these experimental difficulties during this pair of tests, the tests were still kept for analysis, since they let appear a new family of compounds, deriving from the late injection of hydrogen. For these tests, the history of concentration for each oligomer population was plotted as a function of time in Figure 4.8:

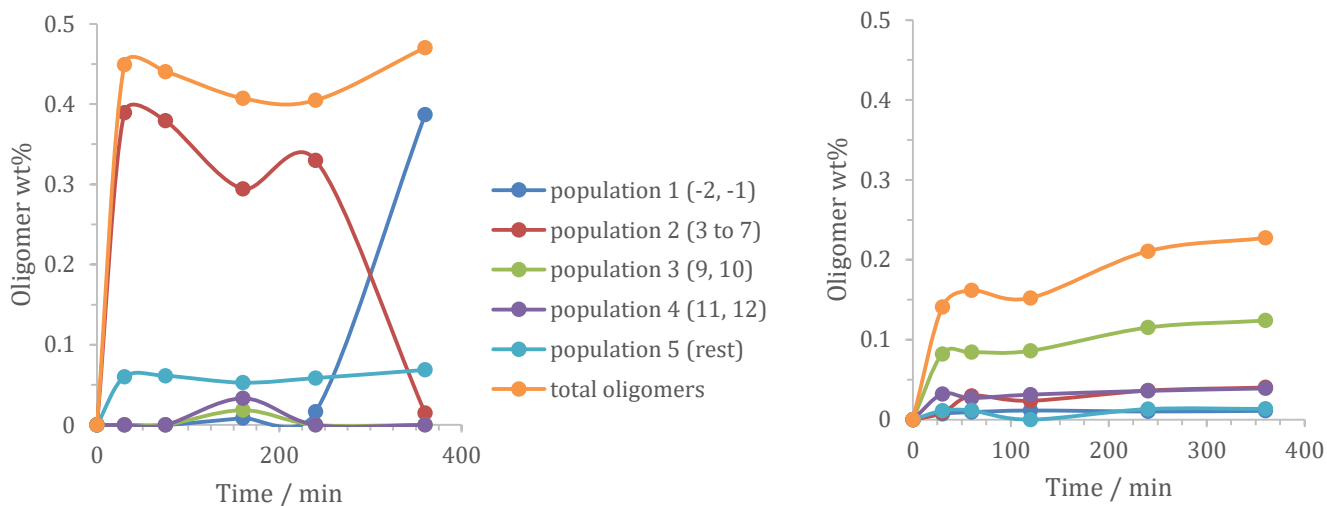


Figure 4.8 - Test 9 (left) and test 10 (right) populations' history.

The results obtained for quantifying the oligomer formation are summarized in Tables 4.16 and 4.17:

Table 4.16 - Obtained results in GC AB for tests 9 and 10.

GC AB Test 9		GC AB Test 10	
oligomer wt%	0.47	oligomer wt%	0.23
oligomer mass / mg	<b>776.58</b>	oligomer mass / mg	<b>398.71</b>

Table 4.17 - Obtained results in TGA and GC-MS for tests 9 and 10.

TGA clear catalyst		TGA dark catalyst		GC-MS	
desorbed mass	3.8%	desorbed mass	4.4%	oligomer wt%	0.01
oligomer mass / mg	<b>95.52</b>	oligomer mass / mg	<b>74.34</b>	sample mass / g	2.52
combusted mass	0.5%	combusted mass	0.7%	oligomer mass / mg	<b>0.15</b>
coke mass / mg	<b>12.09</b>	coke mass / mg	<b>11.31</b>		

## 4.9 Test 11

In order to prevent the catalyst escape event like in the previous runs, from test 11 until test 14 the basket was wrapped by a metal wire that prevented it from opening during the manipulation. The operating conditions that were carried out in this test can be found in Table 4.18:

Table 4.18 - Operating conditions for test 11.

Test	P / barg	T / °C	rpm	Catalyst mass / g	# uses catalyst before	HC mass / g	%H <sub>2</sub> ballast
11	51.0	50.0	560	0.51	0	176.0	0.51% / 100.00%

The effect of having two different ballast compositions is kept studied in this run, and the conditions in which it was achieved the darkest green oil sample were reproduced (test 4).

After realizing that the sampling procedure with the balloons might have a significant impact in the pressure drop over the 6 hours of the batch time (as already discussed in §3.1.5.4), from test 11 until test 14 there were no samples withdrawn during the manipulation, but only in the end of it. For this test, the history of concentration for each oligomer population was plotted as a function of time in Figure 4.9:

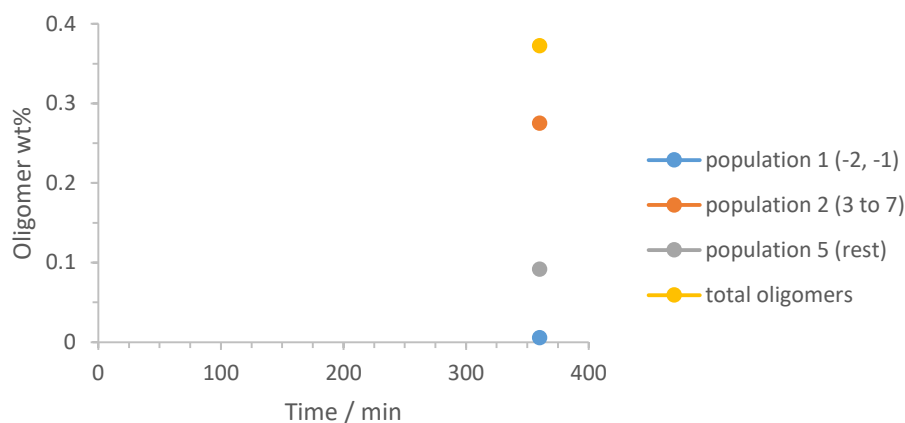


Figure 4.9 - Test 11 populations' history.

The results obtained for quantifying the oligomer formation are summarized in Table 4.19:

Table 4.19 - Obtained results in GC AB, TGA and GC-MS for test 11.

GC AB		TGA		GC-MS	
oligomer wt%	0.37	desorbed mass	3.3%	oligomer wt%	0.39
oligomer mass / mg	655.11	oligomer mass / mg	17.46	sample mass / g	1.45
		combusted mass	0.3%	oligomer mass / mg	5.72
		coke mass / mg	1.53		

## 4.10 Test 12

The operating conditions that were carried out in this test can be found in Table 4.20:

Table 4.20 - Operating conditions for test 12.

Test	P / barg	T / °C	rpm	Catalyst mass / g	# uses catalyst before	HC mass / g	%H <sub>2</sub> ballast
12	50,0	50,0	520	2.01	0	169.7	0.58% / 100.00%

In this test, the same operating conditions as used in the previous test were performed, except that the catalyst mass was four times more as an attempt to achieve a higher oligomer production. For this test, the history of concentration for each oligomer population was plotted as a function of time in Figure 4.10:

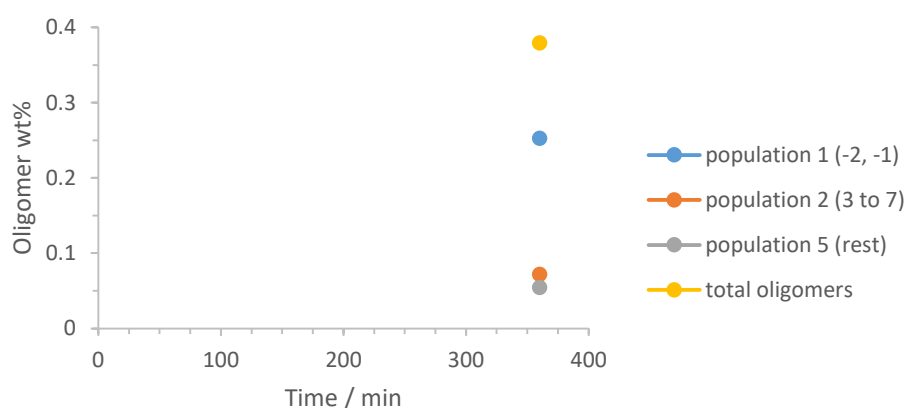


Figure 4.10 - Test 12 populations' history.

The results obtained for quantifying the oligomer formation are summarized in Table 4.21:

Table 4.21 - Obtained results in GC AB, TGA and GC-MS for test 12.

GC AB		TGA		GC-MS	
oligomer wt%	0.38	desorbed mass	1.6%	oligomer wt%	0.29
oligomer mass / mg	644.50	oligomer mass / mg	32.85	sample mass / g	2.44
		combusted mass	0.5%	oligomer mass / mg	7.05
		coke mass / mg	10.10		

#### 4.11 Tests 13 and 14

The operating conditions that were carried out in these tests can be found in Table 4.22:

Table 4.22 - Operating conditions for tests 13 and 14.

Test	P / barg	T / °C	rpm	Catalyst mass / g	# uses catalyst before	HC mass / g	%H <sub>2</sub> ballast
13	51,0	50,0	550	0.50	0	162.2	2.33%
14	51,0	50,0	540	0.50	1	169.1	2.35%

After realizing that the procedure of having two different ballast compositions was not giving satisfactory results towards the production of green oil, that procedure was discarded. The conditions which resulted in the darkest green oil were identically reproduced (test 4), in order to test the repeatability of the overall protocol. For these tests, the history of concentration for each oligomer population was plotted as a function of time in Figure 4.11:

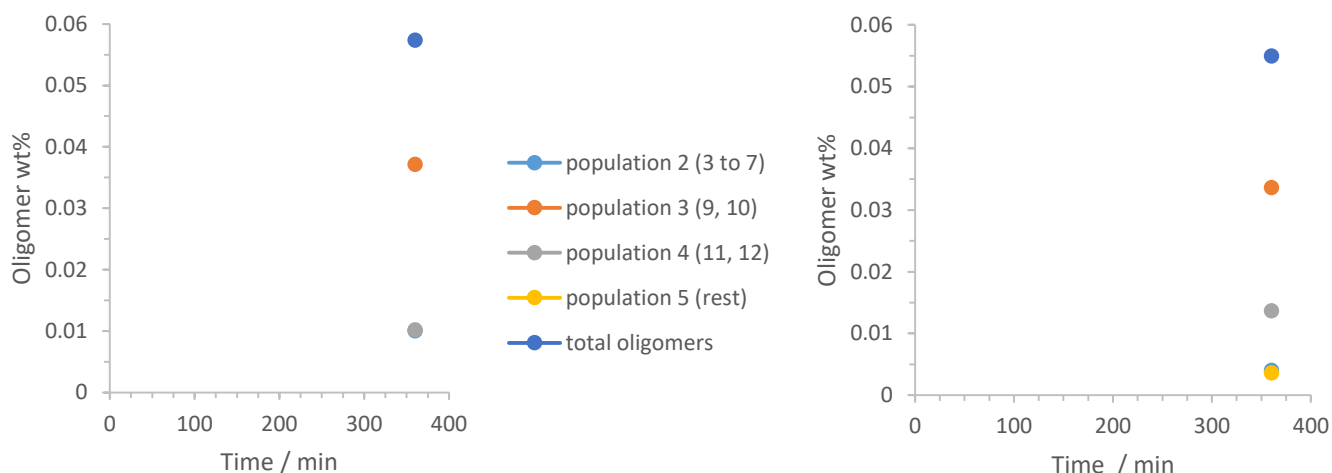


Figure 4.11 - Test 13 (left) and test 14 (right) populations' history.

The results obtained for quantifying the oligomer formation are summarized in Tables 4.23 and 4.24:

Table 4.23 - Obtained results in GC AB for tests 13 and 14.

GC AB Test 13		GC AB Test 14	
oligomer wt%	$5.74 \times 10^{-2}$	oligomer wt%	$5.49 \times 10^{-2}$
oligomer mass / mg	<b>93.08</b>	oligomer mass / mg	<b>92.88</b>

Table 4.24 - Obtained results in TGA and GC-MS for tests 13 and 14.

TGA		GC-MS	
desorbed mass	2.5%	oligomer wt%	0.46
oligomer mass / mg	<b>12.87</b>	sample mass / g	2.51
combusted mass	0.4%	oligomer mass / mg	<b>11.56</b>
coke mass / mg	<b>2.01</b>		

## 5 Discussion

From the literature, one can understand that the operating condition that influences the most the oligomerization reaction is the hydrogen partial pressure in the mixture. Due to the extremely low values that this condition requires to be operated with, it was naturally the most difficult operating condition to be controlled. However, the experimental setup shows successfully to be able to induce and analyze extremely low enough amounts of hydrogen.

From the general results, one can affirm that there are still some operating conditions that were not fully sensitized enough. In the range of the conditions experimented, the oligomer formation kinetics doesn't seem to change with the modification of the hydrogen partial pressure. Which might mean that other tests should be made outside this range, eventually at higher content of hydrogen. Another operating condition that was not sensitized was the temperature factor. Only a few runs with a temperature different from 50 °C were performed, and a more varied data could give us possibly additional information, as for example the activation energies of the oligomerization reactions. Another not fully sensitized aspect was the remaining MAPD. No experiment was conducted that would allow a full discrimination of the oligomerization reactants, i.e., if indeed propylene also contributes to the reaction or if it is only the MAPD portion.

For each "GC AB" analysis separately, the total mass percentage of oligomers formed of a specific sample was calculated as well as the MAPD conversion in the same sample. The results were separated in hydrogenation conditions (test 1) and oligomerization conditions (every other test). In Figure 5.1, the results performed in oligomerization conditions are shown.

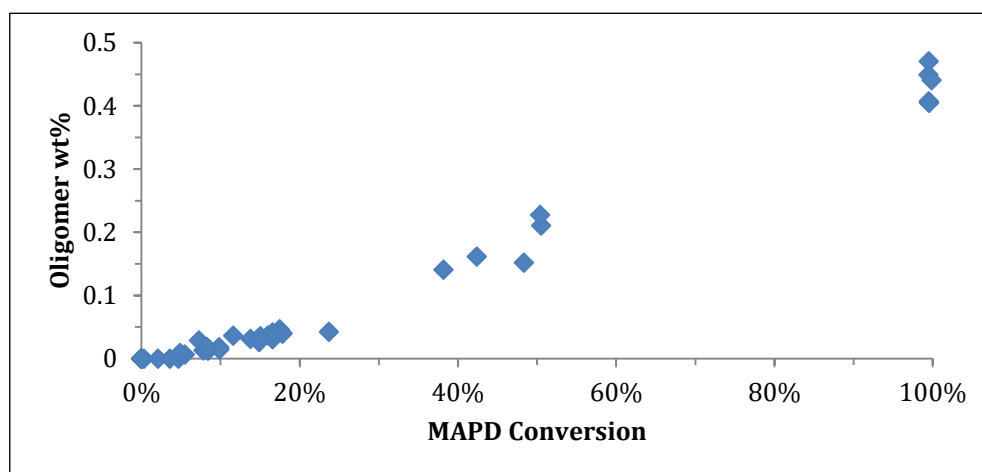


Figure 5.1 - Total C<sub>6</sub> to C<sub>8</sub> as a function of MAPD conversion for oligomerization conditions.

It can be observed that the majority of the runs were performed with low-to-medium MAPD conversion which is satisfactory since high MAPD conversion (that can also be seen in the plot)

means that the hydrogenation of these molecules is happening instead of the preferred oligomerization. We managed our operating conditions from the simulation, in order for the hydrogenation reaction to be moderate (below 50% of MAPD converted), which is what experimentally happened in the majority of the runs, thus we are satisfied by it. On the other hand, we could observe that the C<sub>6</sub>-C<sub>8</sub> oligomer amount in the liquid phase is correlated with the MAPD conversion. Since we cannot properly follow the MAPD hydrogenation by the propylene concentration (it is too high and has no good differential quantification), neither by following the hydrogen consumption (leaks on the H<sub>2</sub> ballast), we cannot directly evaluate which fraction of the MAPD conversion was by hydrogenation or oligomerization. However, from the oligomer analysis, we can evaluate a minimum and a maximum of MAPD conversion to oligomers (either MAPD plus propylene or MAPD plus MAPD respectively), and thus determine by difference the amount of MAPD conversion to propylene.

Looking first at the oligomerization conditions data, the plot seems to show a homogeneous behaviour for every test, which is somewhat unexpected, since we changed the operating conditions especially to create differences. We can observe a linear tendency where the total oligomer weight fraction increases as the MAPD conversion also increases. Then this probably indicates that in the range of the operating conditions performed, the oligomerization kinetics is similar, and the oligomers can be considered as primary products of the reaction of MAPD (no need to consider any intermediate).

One conclusion that can be also reported from test 9 (Table A1.1) is that after full MAPD conversion, there is no more C<sub>6</sub>-C<sub>8</sub> oligomer production. Which is coherent with the literature that affirms that despite not knowing whether the propylene reacts in the oligomerization or not, it is sure that the MAPD is essential for its occurrence.

In order to have just an idea of the impact of the operating temperature in the total C<sub>6</sub>-C<sub>8</sub> oligomer mass fraction, two tests performed at similar conditions were compared being one at 40 °C (test 3) and the other at 50 °C (test 13). Figure 5.2 illustrates those results:

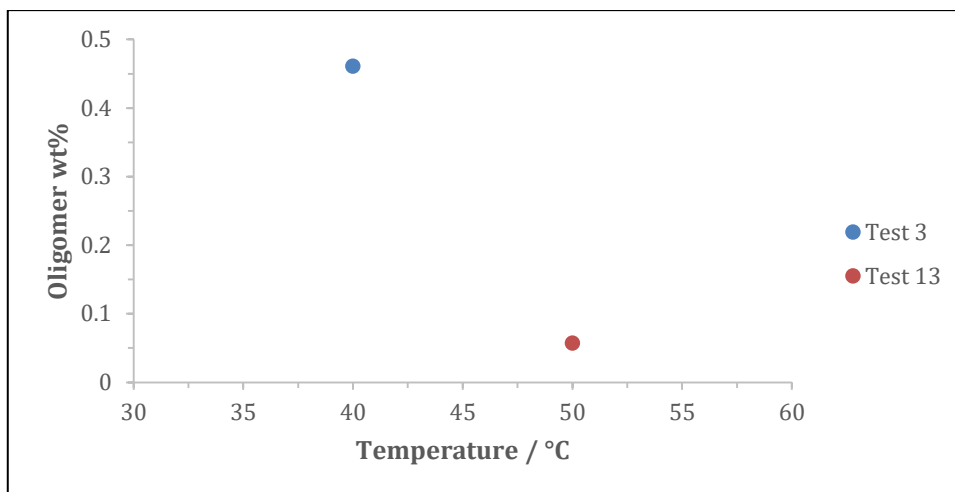


Figure 5.2 - C<sub>6</sub> to C<sub>8</sub> oligomers as a function of temperature of tests 3 and 13.

From the plot, it is possible to observe that the total oligomer C<sub>6</sub>-C<sub>8</sub> weight fraction drops by a factor of 8 just by increasing 10 °C. More different operating temperatures should be tested in order to try to observe some correlated temperature dependence of oligomer concentration in the liquid phase. At the same time, in the end of test 3, 99.5% of MAPD conversion was achieved, whereas for test 13, only 17.7% of conversion. This goes according to the observed trend (already shown) that the content of oligomers seems correlated to the MAPD conversion. Despite the similar conditions, these two tests had significantly different MAPD conversions as already mentioned. This fact, might be due to some H<sub>2</sub> boosts that probably happened in test 3, leading thus to the hydrogenation of MAPD. Since for this test, only the last GC analysis at 360 minutes (Table A1.3) is available, there is no way to confirm this theory with the obtained results. Once again, this reflects the instability of the controlled flow of H<sub>2</sub> in the U865 unit.

In order to extrapolate some tendencies between the different oligomers produced, the oligomer families obtained in each sample are plotted as a function of MAPD conversion in Figure 5.3. In this plot only the families 2, 3 and 4 are shown since they gather most of the oligomer mass and are the only ones displaying variations with conversion and/or operating conditions.

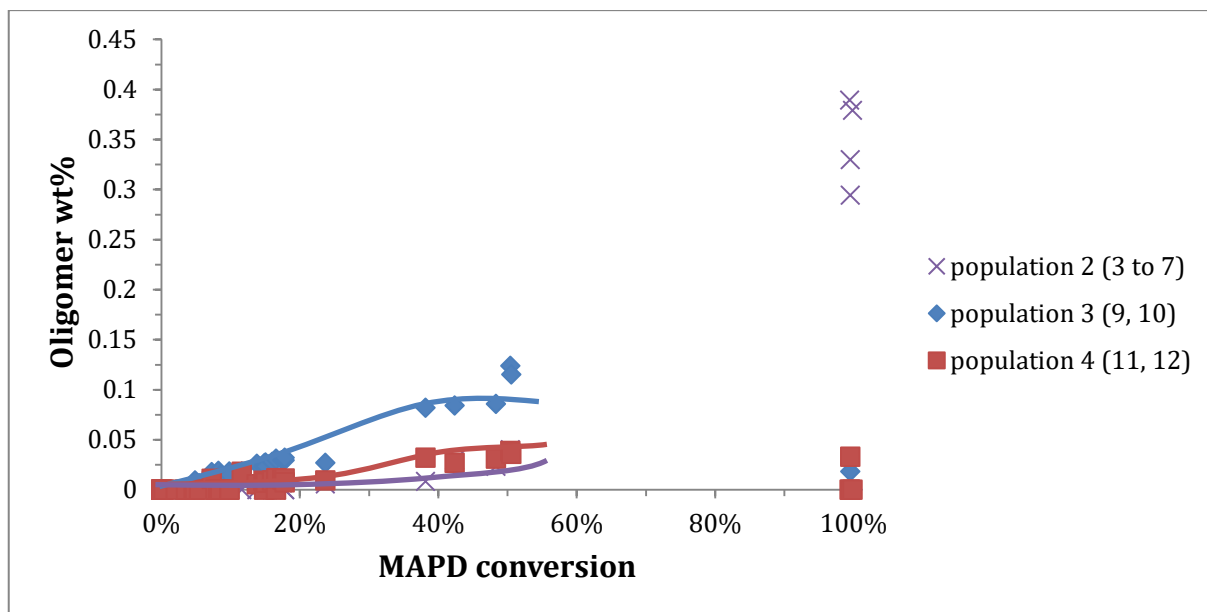


Figure 5.3 - C<sub>6</sub> to C<sub>8</sub> total oligomers divided in populations as a function of MAPD conversion.

The families 3 and 4, i.e., the oligomers 9 and 10 and the oligomers 11 and 12, seem to behave in a similar manner. They start with a low wt% since the MAPD conversion is also low, thus not able to produce more oligomers. These families seem to be produced as primary products, since they already appear at very low MAPD conversion. Besides, since in our tests they appear correlated, they could also be lumped together, although they appear at significantly different retention times. Actually, very different C<sub>6</sub> structures can be produced out of MAPD oligomerization, leading to very different retention times depending mostly on the polarity. More tests should be executed with medium-to-full MAPD conversion in order to have a better representation of the oligomer families' concentration in this area, and in order to observe more discriminating behaviour between populations 3 and 4.

As already explained in the subchapter 4.8, the test 9 had some serious operating problems, one of them being a significant pressure drop inside the reactor. In order to compensate it, the pure hydrogen ballast was used, thus the hydrogen concentration inside the reactor increased importantly between 240 and 360 minutes run time. The several oligomer families that were found in this test, as well as the total amount of oligomers produced in this test are plotted in Figure 4.8 as a function of the run time. The first interesting observation that should be highlighted is the appearance of a new oligomer family that didn't show up in significant concentrations in the previous tests: the oligomer family 1, i.e., the oligomers -2, -1 and 0. Their concentration is almost none during the test, until the hydrogen boost occurs (verified by the "GC H<sub>2</sub>" analysis) and so it seems that it provoked also a boost in family 1 concentration. On the other hand, the oligomer family 2 concentration was pretty high during the experimental test, until the hydrogen boost occurred leading to a complete extinction of this family. The oligomer family 1 formation could not come from the direct conversion of MAPD since for this

test, at 30 minutes, there was already achieved a 99.5% conversion of MAPD. From the simple mass balance between the last samples, one can only postulate that the oligomer family 2 is being transformed into the oligomer family 1, most probably by hydrogenation.

From these results, two different oligomerization mechanisms are proposed: one acting in series, and another one in parallel. In Figures 5.4 and 5.5, the oligomerization mechanisms in series and in parallel are represented, respectively:

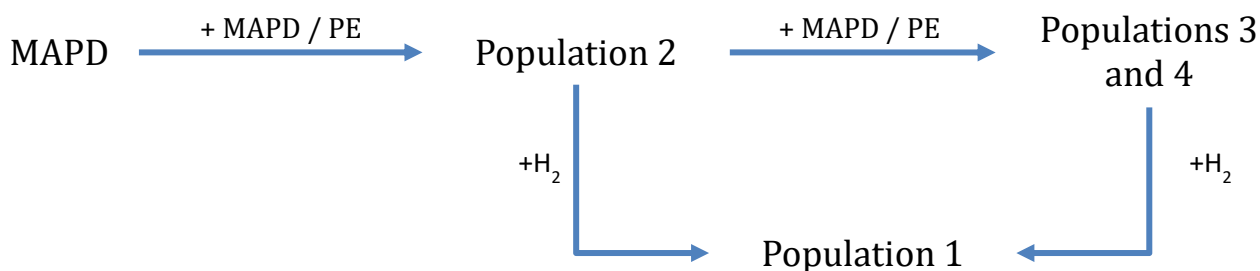


Figure 5.4 - Proposed reaction mechanism in series.

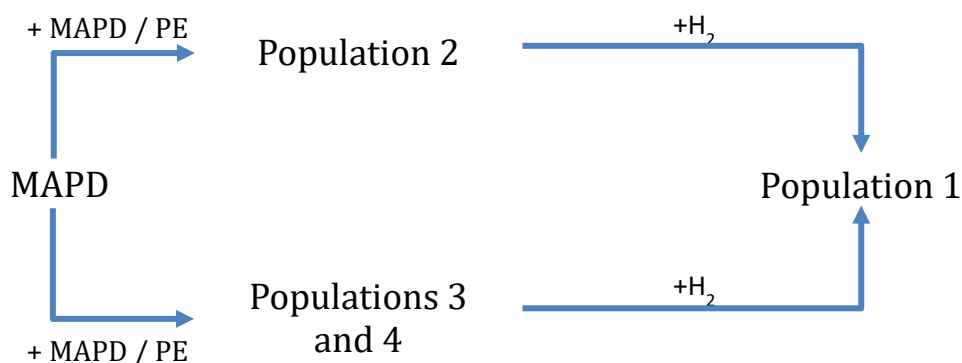


Figure 5.5 - Proposed reaction mechanism in parallel.

No experiment was conducted that would allow to discriminate between the series or the parallel mechanisms towards the different families that were reported. In this case, one can try to fit both schemes into a mathematical model, and then see which one is the most coherent with the data. We could also suggest other experiments in order to be able to discriminate the points mentioned above, for example, experiments with MAPD isotopic carbons and their tracking. Čermák et al. (1987) used isotopic tracking of MAPD in their study, however, only MAPD was used as reactant and no propylene was present.

Similarly, as already presented in Figure 5.1, the total mass percentage of C<sub>6</sub>-C<sub>8</sub> oligomers, in hydrogenation conditions (test 1), is presented in Figure 5.6:

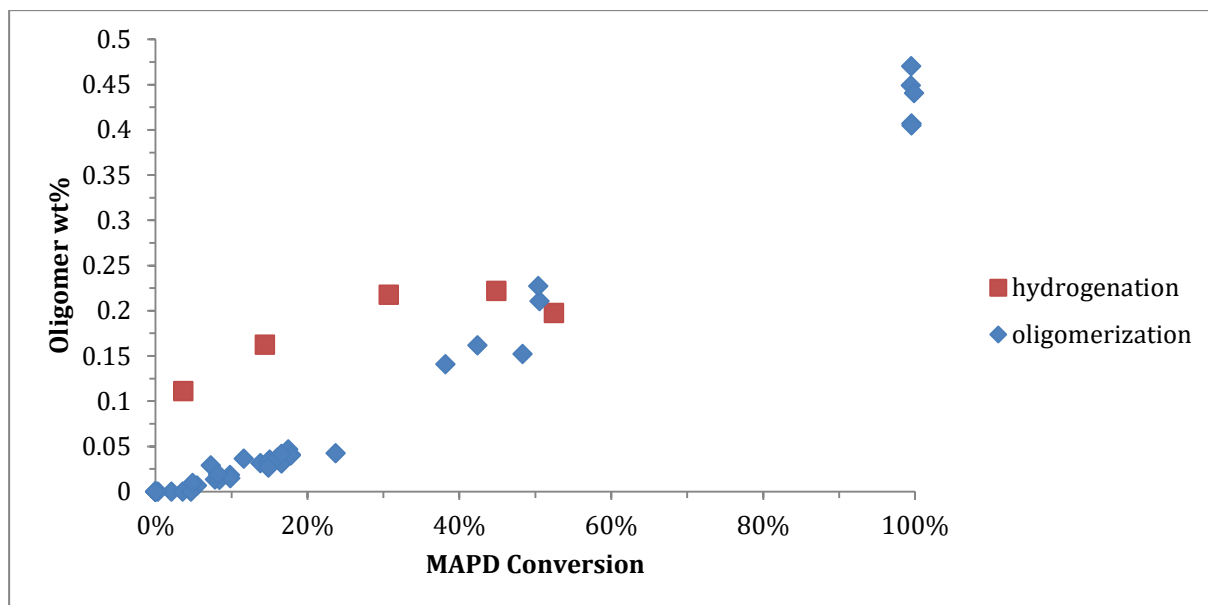


Figure 5.6 - Total C<sub>6</sub> to C<sub>8</sub> oligomers as a function of MAPD conversion.

Observing the 5 samples taken in test 1, the oligomer mass fraction is increasing until the third sample, and then stabilizes and eventually decreases. For these operating conditions, the total C<sub>6</sub>-C<sub>8</sub> oligomer weight fraction does not seem to behave as the trend observed as in oligomerization conditions. This difference in global amounts of oligomer compounds might indicate the presence of a different oligomerization mechanism in hydrogenation conditions. This operating condition was however not reproduced, and any conclusion concerning this “hydrogenation conditions” still needs to be confirmed. Besides, one should keep in mind that these results only consider the oligomers C<sub>6</sub> to C<sub>8</sub>. Which means that a low wt% of these oligomers does not exclude a higher overall oligomer content due to the possibility of having a substantial heavier oligomers content (green oil), and vice-versa. The fact that, from the fourth to the fifth sample of test 1 the oligomer wt% decreases might be due to the mass losses in the sampling procedure, or that those oligomers are reacting towards even higher chain molecules, thus producing green oil. More runs in hydrogenation conditions should be performed in order to provide a better understanding of this tendency.

## 6 Conclusion

The oligomerization of the C<sub>3</sub>-cut in liquid phase was studied in the already described experimental set up, with the objective to gather enough valid and useful data in order to be able to model it. From the experiments, 16 different oligomers with 6 to 8 carbons were identified and divided in 5 distinct populations. The concentration gathered can be simulated in a kinetic model and are able to be implemented. Some of this work was carried out, but due to the shortage of an internship time, it was not possible to investigate it deeper.

The concentration of those oligomers seems to have a linear tendency as the MAPD conversion is increased. Even in normal hydrogenation conditions, those oligomers are produced in such an amount that cannot be neglected, since they are produced in a significant extent.

Two reacting mechanisms are proposed, based on the grouping of C<sub>6</sub> to C<sub>8</sub> oligomers into different populations: one in series, and another one in parallel. No experiment was performed that allowed to choose a mechanism, but by implementing the two mechanisms in a mathematical model, one can compare the deviations of the simulated data with the experimental data, and possibly draw a conclusion.

The operating protocol seems to impact strongly the results since the sampling procedure provokes significant losses of pressure over the run time, each time that a sampling balloon is utilized. Also, the condensation of some of the heavier oligomers present in the balloon, will induce an underestimation of their true concentration. In order to solve these obstacles, online analysis of the oligomers in the liquid phase is recommended to be implemented in the U865 unit.

## 7 Assessment of the work done

### 7.1 Objectives Achieved

The operating conditions were changed across this project, and for each test, it was possible to quantify until some extent, the oligomer content that was produced. With the gathered data is then possible to propose some mechanisms, which was done, and even implement the oligomerization mechanism in an already existing model for the selective hydrogenation. This later part was not concluded. It was also possible to evaluate the functionality of each tool of the experimental set up for the topic studied.

### 7.2 Other Work Carried Out

In order to be more time-effective, two VBA sub-routines were developed that would perform a primary data treatment of the two GCs' results from a text file, and would present a new treated table in an excel file. Also, the initial used simulator for evaluating the operating conditions was adapted in order to take into account the oligomerization reactions and a few simulations were performed.

### 7.3 Limitations and Future Work

If further similar experiments are going to be carried out in the same unit, the implementation of online analysis is recommended as well as an automatic pressure controller between the ballast and the reactor. Longer batch times should be carried out for trying to produce heavier oligomers, but in order to do so, another unit should be used since the U865 lacks of night surveillance. The green-oil recovery method should be compared with other protocols using termination, opening, or washing of the catalyst.

### 7.4 Final Assessment

Due to the complexity of the oligomerization reactions of the C<sub>3</sub>-cut, the developed work seems to be a small step on the research of the topic. Nonetheless, the obtained results can now be used as a starting point for further related works performed at IFPen. In this research center I had the possibility to work with several good professionals from laboratory technicians to modeling engineers. Working in an international environment allowed me to get acquainted to a new language (French) and get in touch with different cultures and different ways of thinking, which will benefit my professional career.

## References

- Bond, G.C., Sheridan, J. Studies in Heterogeneous Catalysis Part 2 - The Hydrogenation of Allene. Transactions of the Faraday Society, **48**, 658-663 (1952).
- Borodziński, A., Cybulski, A. A Kinetic Model of Hydrogenation of Acetylene-Ethylene Mixtures Over a Palladium Surface Covered by Carbonaceous Deposits. Applied Catalysis A: General, **198**, 51-66 (2000).
- Bos, A.N.R., Westerterp, K.R. Mechanism and Kinetics of the Selective Hydrogenation of Ethyne and Ethene. Chemical Engineering and Processing, **32**, 1-7 (1993).
- Braga, M. *Étude des Phénomènes de Transfert et de l'Hydrodynamique dans des Réacteurs Agités à Panier Catalytique*. PhD final thesis, Université Claude Bernard, Lyon, France, 2015.
- Bridier, B., Lopez, N., Pérez-Ramírez, J. Molecular Understanding of Alkyne Hydrogenation for the Design of Selective Catalysts. Dalton Transactions, **39**, 8412-8419 (2010).
- Čermák, J., Blechta, V., Chvalovský, V. Cooligomerization of Propadiene with Propyne Catalysed by Nickel(0) Complexes. Collection of Czechoslovak Communications, **53**, 1274-1286 (1998).
- Friedrich, M.F., Lucas, M., Claus, P. Selective Hydrogenation of Propyne on a Solid Pd/Al<sub>2</sub>O<sub>3</sub> Catalyst Modified With Ionic Liquid Layer (SCILL). Catalysis Communications, **88**, 73-76 (2017).
- Mary, G., Esmaeili, A., Chaouki, J. Simulation of the Selective Hydrogenation of C<sub>3</sub>-cut in the Liquid Phase. International Journal of Chemical Reactor Engineering, **14**, (2016).
- McCue, A.J., Gibson, A., Anderson, J.A. Palladium Assisted Copper/Alumina Catalysts for the Selective Hydrogenation of Propyne, Propadiene and Propene Mixed Feeds. Chemical Engineering Journal, **285**, 384-391 (2016).
- Teixeira, M., Madeira, L.M., Sousa, J.M., Mendes, A. Improving Propyne Removal From Propylene Streams Using a Catalytic Membrane Reactor - a Theoretical Study. Journal of Membrane Science, **375**, 124-133 (2011).
- Wang, B., Froment, G.F. Kinetic Modeling and Simulation of the Selective Hydrogenation of the C<sub>3</sub>-cut of a Thermal Cracking Unit. Industrial & Engineering Chemistry Research, **44**, 9860-9867 (2005).

## Appendix 1 Rescaled results of GC AB and GC H<sub>2</sub>

Table A1.1 - GCs' rescaled results for test 1.

Time / min	15	30	60	100	120
Hydrogen	$2.54 \times 10^{-1}$	$3.43 \times 10^{-1}$	$2.10 \times 10^{-1}$	$9.60 \times 10^{-2}$	$4.18 \times 10^{-2}$
Nitrogen	$7.59 \times 10^0$	$2.01 \times 10^0$	$1.89 \times 10^0$	$4.87 \times 10^0$	$9.35 \times 10^0$
MA	$1.03 \times 10^0$	$9.47 \times 10^{-1}$	$7.17 \times 10^{-1}$	$5.14 \times 10^{-1}$	$3.87 \times 10^{-1}$
PD	$8.54 \times 10^{-1}$	$8.43 \times 10^{-1}$	$7.42 \times 10^{-1}$	$6.14 \times 10^{-1}$	$5.29 \times 10^{-1}$
Propylene	$8.24 \times 10^1$	$8.84 \times 10^1$	$8.93 \times 10^1$	$8.70 \times 10^1$	$8.21 \times 10^1$
Propane	$3.50 \times 10^0$	$3.71 \times 10^0$	$3.77 \times 10^0$	$3.64 \times 10^0$	$3.45 \times 10^0$
Oligo population 1	$0.00 \times 10^0$	$0.00 \times 10^0$	$0.00 \times 10^0$	$0.00 \times 10^0$	$0.00 \times 10^0$
Oligo population 2	$6.97 \times 10^{-2}$	$8.33 \times 10^{-2}$	$9.91 \times 10^{-2}$	$9.76 \times 10^{-2}$	$9.04 \times 10^{-2}$
Oligo population 3	$2.91 \times 10^{-2}$	$4.89 \times 10^{-2}$	$7.78 \times 10^{-2}$	$8.46 \times 10^{-2}$	$7.09 \times 10^{-2}$
Oligo population 4	$0.00 \times 10^0$	$1.27 \times 10^{-2}$	$1.51 \times 10^{-2}$	$1.95 \times 10^{-2}$	$1.74 \times 10^{-2}$
Oligo population 5	$1.24 \times 10^{-2}$	$1.76 \times 10^{-2}$	$2.55 \times 10^{-2}$	$2.03 \times 10^{-2}$	$1.87 \times 10^{-2}$
Total oligomers	$1.11 \times 10^{-1}$	$1.63 \times 10^{-1}$	$2.18 \times 10^{-1}$	$2.22 \times 10^{-1}$	$1.97 \times 10^{-1}$

Table A1.2 - GCs' rescaled results for test 2.

Time / min	0	30	60	120
Hydrogen	$3.45 \times 10^{-3}$	$2.57 \times 10^{-2}$	$4.34 \times 10^{-2}$	$1.74 \times 10^{-2}$
Nitrogen	$3.27 \times 10^{-2}$	$1.26 \times 10^1$	$5.41 \times 10^0$	$5.78 \times 10^0$
MA	$1.32 \times 10^0$	$1.10 \times 10^0$	$1.18 \times 10^0$	$1.13 \times 10^0$
PD	$1.05 \times 10^0$	$8.74 \times 10^{-1}$	$9.68 \times 10^{-1}$	$9.38 \times 10^{-1}$
Propylene	$9.12 \times 10^1$	$7.80 \times 10^1$	$8.62 \times 10^1$	$8.45 \times 10^1$
Propane	$3.87 \times 10^0$	$3.29 \times 10^0$	$3.64 \times 10^0$	$3.58 \times 10^0$
Oligo population 1	$0.00 \times 10^0$	$0.00 \times 10^0$	$0.00 \times 10^0$	$0.00 \times 10^0$
Oligo population 2	$0.00 \times 10^0$	$0.00 \times 10^0$	$0.00 \times 10^0$	$0.00 \times 10^0$
Oligo population 3	$0.00 \times 10^0$	$0.00 \times 10^0$	$0.00 \times 10^0$	$6.50 \times 10^{-3}$
Oligo population 4	$0.00 \times 10^0$	$0.00 \times 10^0$	$0.00 \times 10^0$	$0.00 \times 10^0$
Oligo population 5	$0.00 \times 10^0$	$0.00 \times 10^0$	$0.00 \times 10^0$	$0.00 \times 10^0$
Total oligomers	$0.00 \times 10^0$	$0.00 \times 10^0$	$0.00 \times 10^0$	$6.50 \times 10^{-3}$

Table A1.3 - GCs' rescaled results for test 3.

<b>Time / min</b>	<b>360</b>
<b>Hydrogen</b>	$1.27 \times 10^{-1}$
<b>Nitrogen</b>	$6.54 \times 10^0$
<b>MA</b>	$6.80 \times 10^{-3}$
<b>PD</b>	$4.10 \times 10^{-3}$
<b>Propylene</b>	$8.48 \times 10^1$
<b>Propane</b>	$6.80 \times 10^0$
<b>Oligo population 1</b>	$0.00 \times 10^0$
<b>Oligo population 2</b>	$3.95 \times 10^{-1}$
<b>Oligo population 3</b>	$0.00 \times 10^0$
<b>Oligo population 4</b>	$0.00 \times 10^0$
<b>Oligo population 5</b>	$6.62 \times 10^{-2}$
<b>Total oligomers</b>	$4.61 \times 10^{-1}$

Table A1.4 - GCs' rescaled results for test 4.

<b>Time / min</b>	<b>0</b>	<b>60</b>	<b>120</b>	<b>180</b>	<b>270</b>	<b>360</b>
<b>Hydrogen</b>	$7.56 \times 10^{-3}$	$4.66 \times 10^{-2}$	$1.66 \times 10^{-2}$	$6.10 \times 10^{-3}$	$1.60 \times 10^{-3}$	$1.59 \times 10^{-3}$
<b>Nitrogen</b>	$4.97 \times 10^{-1}$	$8.21 \times 10^0$	$7.71 \times 10^0$	$7.99 \times 10^0$	$7.59 \times 10^0$	$7.51 \times 10^0$
<b>MA</b>	$1.21 \times 10^0$	$9.59 \times 10^{-1}$	$8.91 \times 10^{-1}$	$8.53 \times 10^{-1}$	$8.75 \times 10^{-1}$	$8.49 \times 10^{-1}$
<b>PD</b>	$9.94 \times 10^{-1}$	$8.85 \times 10^{-1}$	$8.26 \times 10^{-1}$	$8.27 \times 10^{-1}$	$8.47 \times 10^{-1}$	$8.36 \times 10^{-1}$
<b>Propylene</b>	$9.10 \times 10^1$	$8.23 \times 10^1$	$8.26 \times 10^1$	$8.20 \times 10^1$	$8.38 \times 10^1$	$8.23 \times 10^1$
<b>Propane</b>	$3.84 \times 10^0$	$3.45 \times 10^0$	$3.48 \times 10^0$	$3.45 \times 10^0$	$3.54 \times 10^0$	$3.46 \times 10^0$
<b>Oligo population 1</b>	$0.00 \times 10^0$	$0.00 \times 10^0$	$0.00 \times 10^0$	$0.00 \times 10^0$	$0.00 \times 10^0$	$0.00 \times 10^0$
<b>Oligo population 2</b>	$0.00 \times 10^0$	$0.00 \times 10^0$	$0.00 \times 10^0$	$0.00 \times 10^0$	$0.00 \times 10^0$	$0.00 \times 10^0$
<b>Oligo population 3</b>	$0.00 \times 10^0$	$1.78 \times 10^{-2}$	$2.61 \times 10^{-2}$	$2.34 \times 10^{-2}$	$2.34 \times 10^{-2}$	$2.74 \times 10^{-2}$
<b>Oligo population 4</b>	$0.00 \times 10^0$	$1.10 \times 10^{-2}$	$5.52 \times 10^{-3}$	$7.28 \times 10^{-3}$	$9.17 \times 10^{-3}$	$8.07 \times 10^{-3}$
<b>Oligo population 5</b>	$0.00 \times 10^0$	$0.00 \times 10^0$	$0.00 \times 10^0$	$0.00 \times 10^0$	$0.00 \times 10^0$	$0.00 \times 10^0$
<b>Total oligomers</b>	$0.00 \times 10^0$	$2.88 \times 10^{-2}$	$3.16 \times 10^{-2}$	$3.07 \times 10^{-2}$	$3.26 \times 10^{-2}$	$3.54 \times 10^{-2}$

Table A1.5 - GCs' rescaled results for test 5.

Time / min	30	75	135	210	285	360
Hydrogen	$4.76 \times 10^{-2}$	$8.66 \times 10^{-3}$	$2.28 \times 10^{-2}$	$0.00 \times 10^0$	$2.07 \times 10^{-3}$	$2.11 \times 10^{-3}$
Nitrogen	$7.74 \times 10^0$	$7.11 \times 10^0$	$7.20 \times 10^0$	$0.00 \times 10^0$	$7.31 \times 10^0$	$6.52 \times 10^0$
MA	$1.06 \times 10^0$	$9.87 \times 10^{-1}$	$8.97 \times 10^{-1}$	$0.00 \times 10^0$	$8.74 \times 10^{-1}$	$8.04 \times 10^{-1}$
PD	$8.76 \times 10^{-1}$	$8.70 \times 10^{-1}$	$8.32 \times 10^{-1}$	$0.00 \times 10^0$	$8.47 \times 10^{-1}$	$8.05 \times 10^{-1}$
Propylene	$8.23 \times 10^1$	$8.31 \times 10^1$	$8.29 \times 10^1$	$0.00 \times 10^0$	$8.37 \times 10^1$	$8.38 \times 10^1$
Propane	$3.46 \times 10^0$	$3.49 \times 10^0$	$3.55 \times 10^0$	$0.00 \times 10^0$	$3.51 \times 10^0$	$3.36 \times 10^0$
Oligo population 1	$0.00 \times 10^0$	$0.00 \times 10^0$	$0.00 \times 10^0$	$0.00 \times 10^0$	$0.00 \times 10^0$	$0.00 \times 10^0$
Oligo population 2	$0.00 \times 10^0$	$0.00 \times 10^0$	$0.00 \times 10^0$	$0.00 \times 10^0$	$0.00 \times 10^0$	$5.91 \times 10^{-3}$
Oligo population 3	$0.00 \times 10^0$	$1.83 \times 10^{-2}$	$3.11 \times 10^{-2}$	$0.00 \times 10^0$	$2.97 \times 10^{-2}$	$2.70 \times 10^{-2}$
Oligo population 4	$0.00 \times 10^0$	$0.00 \times 10^0$	$0.00 \times 10^0$	$0.00 \times 10^0$	$1.14 \times 10^{-2}$	$9.56 \times 10^{-3}$
Oligo population 5	$0.00 \times 10^0$	$0.00 \times 10^0$	$0.00 \times 10^0$	$0.00 \times 10^0$	$0.00 \times 10^0$	$0.00 \times 10^0$
Total oligomers	$0.00 \times 10^0$	$1.83 \times 10^{-2}$	$3.11 \times 10^{-2}$	$0.00 \times 10^0$	$4.10 \times 10^{-2}$	$4.25 \times 10^{-2}$

Table A1.6 - GCs' rescaled results for test 6.

Time / min	0	30	75	135	210	285	360
Hydrogen	$0.00 \times 10^0$	$3.19 \times 10^{-2}$	$3.66 \times 10^{-2}$	$1.44 \times 10^{-2}$	$4.74 \times 10^{-3}$	$2.37 \times 10^{-3}$	$2.43 \times 10^{-3}$
Nitrogen	$0.00 \times 10^0$	$6.65 \times 10^0$	$6.98 \times 10^0$	$6.64 \times 10^0$	$7.01 \times 10^0$	$7.21 \times 10^0$	$7.29 \times 10^0$
MA	$1.23 \times 10^0$	$1.06 \times 10^0$	$9.45 \times 10^{-1}$	$9.00 \times 10^{-1}$	$9.03 \times 10^{-1}$	$8.59 \times 10^{-1}$	$8.63 \times 10^{-1}$
PD	$9.87 \times 10^{-1}$	$8.81 \times 10^{-1}$	$8.44 \times 10^{-1}$	$8.42 \times 10^{-1}$	$8.54 \times 10^{-1}$	$8.24 \times 10^{-1}$	$8.32 \times 10^{-1}$
Propylene	$9.03 \times 10^1$	$8.31 \times 10^1$	$8.25 \times 10^1$	$8.35 \times 10^1$	$8.54 \times 10^1$	$8.36 \times 10^1$	$8.29 \times 10^1$
Propane	$3.80 \times 10^0$	$3.50 \times 10^0$	$3.48 \times 10^0$	$3.51 \times 10^0$	$3.59 \times 10^0$	$3.54 \times 10^0$	$3.49 \times 10^0$
Oligo population 1	$0.00 \times 10^0$	$0.00 \times 10^0$	$0.00 \times 10^0$	$0.00 \times 10^0$	$0.00 \times 10^0$	$0.00 \times 10^0$	$0.00 \times 10^0$
Oligo population 2	$0.00 \times 10^0$	$0.00 \times 10^0$	$0.00 \times 10^0$	$0.00 \times 10^0$	$0.00 \times 10^0$	$0.00 \times 10^0$	$0.00 \times 10^0$
Oligo population 3	$0.00 \times 10^0$	$9.43 \times 10^{-3}$	$1.83 \times 10^{-2}$	$2.65 \times 10^{-2}$	$2.80 \times 10^{-2}$	$3.21 \times 10^{-2}$	$3.02 \times 10^{-2}$
Oligo population 4	$0.00 \times 10^0$	$0.00 \times 10^0$	$1.80 \times 10^{-2}$	$0.00 \times 10^0$	$9.31 \times 10^{-3}$	$7.62 \times 10^{-3}$	$1.16 \times 10^{-2}$
Oligo population 5	$0.00 \times 10^0$	$0.00 \times 10^0$	$0.00 \times 10^0$	$0.00 \times 10^0$	$0.00 \times 10^0$	$0.00 \times 10^0$	$0.00 \times 10^0$
Total oligomers	$0.00 \times 10^0$	$9.43 \times 10^{-3}$	$3.63 \times 10^{-2}$	$2.65 \times 10^{-2}$	$3.73 \times 10^{-2}$	$3.98 \times 10^{-2}$	$4.18 \times 10^{-2}$

Table A1.7 - GCs' rescaled results for test 7.

Time / min	0	30	75
Hydrogen	0.00×10 <sup>0</sup>	4.00×10 <sup>-3</sup>	0.00×10 <sup>0</sup>
Nytrogen	7.44×10 <sup>-2</sup>	7.59×10 <sup>0</sup>	6.95×10 <sup>0</sup>
MA	1.24×10 <sup>0</sup>	1.18×10 <sup>0</sup>	1.15×10 <sup>0</sup>
PD	9.86×10 <sup>-1</sup>	9.30×10 <sup>-1</sup>	9.14×10 <sup>-1</sup>
Propylene	9.19×10 <sup>1</sup>	8.62×10 <sup>1</sup>	8.57×10 <sup>1</sup>
Propane	3.85×10 <sup>0</sup>	3.61×10 <sup>0</sup>	3.59×10 <sup>0</sup>
Oligo population 1	0.00×10 <sup>0</sup>	0.00×10 <sup>0</sup>	0.00×10 <sup>0</sup>
Oligo population 2	0.00×10 <sup>0</sup>	0.00×10 <sup>0</sup>	0.00×10 <sup>0</sup>
Oligo population 3	0.00×10 <sup>0</sup>	0.00×10 <sup>0</sup>	0.00×10 <sup>0</sup>
Oligo population 4	0.00×10 <sup>0</sup>	0.00×10 <sup>0</sup>	0.00×10 <sup>0</sup>
Oligo population 5	0.00×10 <sup>0</sup>	3.06×10 <sup>-3</sup>	0.00×10 <sup>0</sup>
Total oligomers	0.00×10 <sup>0</sup>	3.06×10 <sup>-3</sup>	0.00×10 <sup>0</sup>

Table A1.8 - GCs' rescaled results for test 8.

Time / min	0	30	70	150	285	360
Hydrogen	6.19×10 <sup>-3</sup>	7.47×10 <sup>-3</sup>	0.00×10 <sup>0</sup>	0.00×10 <sup>0</sup>	0.00×10 <sup>0</sup>	0.00×10 <sup>0</sup>
Nytrogen	1.81×10 <sup>-1</sup>	7.33×10 <sup>0</sup>	1.10×10 <sup>1</sup>	6.63×10 <sup>0</sup>	9.36×10 <sup>0</sup>	7.62×10 <sup>0</sup>
MA	1.26×10 <sup>0</sup>	1.04×10 <sup>0</sup>	9.56×10 <sup>-1</sup>	1.02×10 <sup>0</sup>	9.60×10 <sup>-1</sup>	1.02×10 <sup>0</sup>
PD	9.83×10 <sup>-1</sup>	8.82×10 <sup>-1</sup>	8.14×10 <sup>-1</sup>	8.69×10 <sup>-1</sup>	8.31×10 <sup>-1</sup>	8.81×10 <sup>-1</sup>
Propylene	9.24×10 <sup>1</sup>	8.58×10 <sup>1</sup>	7.97×10 <sup>1</sup>	8.48×10 <sup>1</sup>	8.18×10 <sup>1</sup>	8.53×10 <sup>1</sup>
Propane	3.88×10 <sup>0</sup>	3.59×10 <sup>0</sup>	3.33×10 <sup>0</sup>	3.55×10 <sup>0</sup>	3.44×10 <sup>0</sup>	3.57×10 <sup>0</sup>
Oligo population 1	0.00×10 <sup>0</sup>	0.00×10 <sup>0</sup>	0.00×10 <sup>0</sup>	0.00×10 <sup>0</sup>	0.00×10 <sup>0</sup>	0.00×10 <sup>0</sup>
Oligo population 2	0.00×10 <sup>0</sup>	0.00×10 <sup>0</sup>	0.00×10 <sup>0</sup>	0.00×10 <sup>0</sup>	0.00×10 <sup>0</sup>	0.00×10 <sup>0</sup>
Oligo population 3	0.00×10 <sup>0</sup>	1.32×10 <sup>-2</sup>	1.46×10 <sup>-2</sup>	1.29×10 <sup>-2</sup>	1.49×10 <sup>-2</sup>	1.89×10 <sup>-2</sup>
Oligo population 4	0.00×10 <sup>0</sup>	0.00×10 <sup>0</sup>	0.00×10 <sup>0</sup>	0.00×10 <sup>0</sup>	0.00×10 <sup>0</sup>	0.00×10 <sup>0</sup>
Oligo population 5	0.00×10 <sup>0</sup>	0.00×10 <sup>0</sup>	0.00×10 <sup>0</sup>	0.00×10 <sup>0</sup>	0.00×10 <sup>0</sup>	0.00×10 <sup>0</sup>
Total oligomers	0.00×10 <sup>0</sup>	1.32×10 <sup>-2</sup>	1.46×10 <sup>-2</sup>	1.29×10 <sup>-2</sup>	1.49×10 <sup>-2</sup>	1.89×10 <sup>-2</sup>

Table A1.9 - GCs' rescaled results for test 9.

Time / min	0	30	75	160	240	360
Hydrogen	$3.63 \times 10^{-3}$	$4.48 \times 10^{-1}$	$4.81 \times 10^{-1}$	$8.77 \times 10^{-3}$	$5.93 \times 10^{-1}$	$2.68 \times 10^0$
Nitrogen	$2.55 \times 10^{-1}$	$5.04 \times 10^0$	$5.92 \times 10^0$	$3.96 \times 10^0$	$4.35 \times 10^0$	$3.72 \times 10^0$
MA	$1.25 \times 10^0$	$6.36 \times 10^{-3}$	$0.00 \times 10^0$	$6.81 \times 10^{-3}$	$6.28 \times 10^{-3}$	$5.42 \times 10^{-3}$
PD	$9.71 \times 10^{-1}$	$5.47 \times 10^{-3}$	$2.80 \times 10^{-3}$	$3.61 \times 10^{-3}$	$3.57 \times 10^{-3}$	$5.18 \times 10^{-3}$
Propylene	$9.15 \times 10^1$	$8.18 \times 10^1$	$6.14 \times 10^1$	$3.98 \times 10^1$	$1.69 \times 10^1$	$6.98 \times 10^{-2}$
Propane	$3.84 \times 10^0$	$1.22 \times 10^1$	$3.04 \times 10^1$	$5.47 \times 10^1$	$7.73 \times 10^1$	$9.32 \times 10^1$
Oligo population 1	$0.00 \times 10^0$	$0.00 \times 10^0$	$0.00 \times 10^0$	$8.50 \times 10^{-3}$	$1.65 \times 10^{-2}$	$3.87 \times 10^{-1}$
Oligo population 2	$0.00 \times 10^0$	$3.89 \times 10^{-1}$	$3.79 \times 10^{-1}$	$2.94 \times 10^{-1}$	$3.30 \times 10^{-1}$	$1.50 \times 10^{-2}$
Oligo population 3	$0.00 \times 10^0$	$0.00 \times 10^0$	$0.00 \times 10^0$	$1.84 \times 10^{-2}$	$0.00 \times 10^0$	$0.00 \times 10^0$
Oligo population 4	$0.00 \times 10^0$	$0.00 \times 10^0$	$0.00 \times 10^0$	$3.32 \times 10^{-2}$	$0.00 \times 10^0$	$0.00 \times 10^0$
Oligo population 5	$0.00 \times 10^0$	$5.99 \times 10^{-2}$	$6.14 \times 10^{-2}$	$5.28 \times 10^{-2}$	$5.85 \times 10^{-2}$	$6.87 \times 10^{-2}$
Total oligomers	$0.00 \times 10^0$	$4.49 \times 10^{-1}$	$4.41 \times 10^{-1}$	$4.07 \times 10^{-1}$	$4.05 \times 10^{-1}$	$4.70 \times 10^{-1}$

Table A1.2 - GCs' rescaled results for test 10.

Time / min	0	30	60	120	240	360
Hydrogen	$3.80 \times 10^{-3}$	$1.68 \times 10^{-2}$	$3.30 \times 10^{-3}$	$0.00 \times 10^0$	$0.00 \times 10^0$	$0.00 \times 10^0$
Nitrogen	$4.78 \times 10^0$	$7.46 \times 10^0$	$7.83 \times 10^0$	$1.33 \times 10^1$	$7.38 \times 10^0$	$6.96 \times 10^0$
MA	$1.07 \times 10^0$	$4.75 \times 10^{-1}$	$3.97 \times 10^{-1}$	$2.91 \times 10^{-1}$	$2.85 \times 10^{-1}$	$2.84 \times 10^{-1}$
PD	$8.60 \times 10^{-1}$	$7.24 \times 10^{-1}$	$6.85 \times 10^{-1}$	$5.81 \times 10^{-1}$	$6.42 \times 10^{-1}$	$6.45 \times 10^{-1}$
Propylene	$8.69 \times 10^1$	$8.80 \times 10^1$	$8.53 \times 10^1$	$7.67 \times 10^1$	$8.52 \times 10^1$	$8.52 \times 10^1$
Propane	$3.94 \times 10^0$	$3.72 \times 10^0$	$3.57 \times 10^0$	$3.29 \times 10^0$	$3.56 \times 10^0$	$3.56 \times 10^0$
Oligo population 1	$0.00 \times 10^0$	$7.21 \times 10^{-3}$	$9.32 \times 10^{-3}$	$1.14 \times 10^{-2}$	$1.02 \times 10^{-2}$	$1.10 \times 10^{-2}$
Oligo population 2	$0.00 \times 10^0$	$8.33 \times 10^{-3}$	$2.96 \times 10^{-2}$	$2.36 \times 10^{-2}$	$3.62 \times 10^{-2}$	$4.01 \times 10^{-2}$
Oligo population 3	$0.00 \times 10^0$	$8.22 \times 10^{-2}$	$8.43 \times 10^{-2}$	$8.60 \times 10^{-2}$	$1.15 \times 10^{-1}$	$1.24 \times 10^{-1}$
Oligo population 4	$0.00 \times 10^0$	$3.20 \times 10^{-2}$	$2.71 \times 10^{-2}$	$3.12 \times 10^{-2}$	$3.60 \times 10^{-2}$	$3.90 \times 10^{-2}$
Oligo population 5	$0.00 \times 10^0$	$1.10 \times 10^{-2}$	$1.13 \times 10^{-2}$	$0.00 \times 10^0$	$1.31 \times 10^{-2}$	$1.33 \times 10^{-2}$
Total oligomers	$0.00 \times 10^0$	$1.41 \times 10^{-1}$	$1.62 \times 10^{-1}$	$1.52 \times 10^{-1}$	$2.11 \times 10^{-1}$	$2.27 \times 10^{-1}$

Table A1.3 - GCs' rescaled results for test 11.

Time / min	360
Hydrogen	$1.54 \times 10^0$
Nytrogen	$4.92 \times 10^0$
MA	$0.00 \times 10^0$
PD	$0.00 \times 10^0$
Propylene	$4.85 \times 10^1$
Propane	$4.32 \times 10^1$
Oligo population 1	$5.60 \times 10^{-3}$
Oligo population 2	$2.75 \times 10^{-1}$
Oligo population 3	$0.00 \times 10^0$
Oligo population 4	$0.00 \times 10^0$
Oligo population 5	$9.18 \times 10^{-2}$
Total oligomers	$3.72 \times 10^{-1}$

Table A1.4 - GCs' rescaled results for test 12.

Time / min	360
Hydrogen	$2.44 \times 10^0$
Nytrogen	$5.12 \times 10^0$
MA	$5.50 \times 10^{-3}$
PD	$4.69 \times 10^{-3}$
Propylene	$8.33 \times 10^{-2}$
Propane	$8.77 \times 10^1$
Oligo population 1	$2.53 \times 10^{-1}$
Oligo population 2	$7.21 \times 10^{-2}$
Oligo population 3	$0.00 \times 10^0$
Oligo population 4	$0.00 \times 10^0$
Oligo population 5	$5.47 \times 10^{-2}$
Total oligomers	$3.80 \times 10^{-1}$

Table A1.13 - GCs' obtained results for test 13.

Time / min	360
Hydrogen	0.00×10 <sup>0</sup>
Nytrogen	7.00×10 <sup>0</sup>
MA	8.43×10 <sup>-1</sup>
PD	8.30×10 <sup>-1</sup>
Propylene	8.62×10 <sup>1</sup>
Propane	3.66×10 <sup>0</sup>
Oligo population 1	0.00×10 <sup>0</sup>
Oligo population 2	1.00×10 <sup>-2</sup>
Oligo population 3	3.71×10 <sup>-2</sup>
Oligo population 4	1.02×10 <sup>-2</sup>
Oligo population 5	0.00×10 <sup>0</sup>
Total oligomers	5.74×10 <sup>-2</sup>

Table A1.14 - GCs' obtained results for test 14.

Time / min	360
Hydrogen	0.00×10 <sup>0</sup>
Nytrogen	7.22×10 <sup>0</sup>
MA	8.75×10 <sup>-1</sup>
PD	8.32×10 <sup>-1</sup>
Propylene	8.55×10 <sup>1</sup>
Propane	3.62×10 <sup>0</sup>
Oligo population 1	0.00×10 <sup>0</sup>
Oligo population 2	4.02×10 <sup>-3</sup>
Oligo population 3	3.36×10 <sup>-2</sup>
Oligo population 4	1.37×10 <sup>-2</sup>
Oligo population 5	3.59×10 <sup>-3</sup>
Total oligomers	5.49×10 <sup>-2</sup>

## Appendix 2 Photography of green-oil and catalyst



*Figure A2.1 - Green oil collected in tests 7 and 8.*



*Figure A2.2 - Catalyst after use in tests 7 and 8.*